Physical, Soil, and Paleomagnetic Stratigraphy of the Upper Cenozoic Sediments in Fisher Valley, Southeastern Utah

FRONTISPIECE. Oblique aerial view of Fisher Valley, Utah. View is northwest, down the course of Onion Creek. The floor of Fisher Valley is in the foreground, perched above the erosional amphitheater eroded by the headwaters of Onion Creek into the upper Cenozoic basin-fill deposits. The light-colored rocks in the middle distance are the cap rock of the Onion Creek salt diapir; to the right are Fisher Towers—Permian and Triassic rocks that form the northeast flank of the Fisher Valley anticline. The Colorado River flows southwest (to the left) at the base of the prominent cliffs in the distance. The Salt Valley anticline and Arches National Park are barely visible in the far distance (left).

Physical, Soil, and Paleomagnetic Stratigraphy of the Upper Cenozoic Sediments in Fisher Valley, Southeastern Utah

By STEVEN M. COLMAN, ANNE F. CHOQUETTE, and FRED F. HAWKINS

The sediments and soils in Fisher Valley provide a record of geomorphic changes, deposition, and deformation associated with movement of the Onion Creek salt diapir.

DEPARTMENT OF THE INTERIOR
DONALD PAUL HODEL, Secretary

U.S. GEOLOGICAL SURVEY
Dallas L. Peck, Director

CONTENTS

FIGURES

FIGURES

TABLES

Physical, Soil, and Paleomagnetic Stratigraphy of the Upper Cenozoic Sediments in Fisher Valley, Southeastern Utah

By Steven M. Colman, Anne F. Choquette, *and* Fred F. Hawkins

Abstract

The upper Cenozoic deposits in the Fisher Valley area, Utah, a thick sequence (> 145 m) of basin-fill sediments, contrast markedly with the thin, discontinuous deposits of this age that characterize the erosional terrain of the Paradox basin and the Colorado Plateau province. The sediments in Fisher Valley are second-cycle red beds derived from late Paleozoic and Mesozoic sedimentary bedrock. They are composed of interbedded fluvial and eolian sand, with minor fluvial gravel, which thins and grades into primarily alluvial-fan gravel towards the margins of the depositional basin. The sediments can be divided into depositional subunits that vary in thickness and distinctness and that define crude cycles related to diapiric deformation and climatic change. Each cycle begins with fluvial sands and gravels, grades upward into massive eolian sand, and ends with a period of landscape stability and soil formation. The sediments contain the Lava Creek ash (0.61 m.y.) and the Bishop ash (0.73 m.y.), which form important stratigraphic markers.

The pre-Holocene buried soils interbedded with the Fisher Valley sediments provide important age information for the section. Most of the soils are polygenetic and are better developed than Holocene soils in the area. Assuming that secondary clay and carbonate in these soils are derived primarily from airborne sources and from the original contents of these materials in the sediments, and assuming that long-term rates of addition of these constituents have been constant, it is possible to estimate the age of each soil in the section. Long-term rates of accumulation of secondary carbonate and clay are calibrated by the total amount of these constituents above the stratigraphic markers provided by the Lava Creek and Bishop ashes and the Brunhes-Matuyama paleomagnetic boundary. Ages estimated for the soils by these methods are generally consistent with other independent age estimates. Accordingly, the uppermost buried soil, which marks the end of deposition of the basin-fill sediments, began to form about 0.25 m.y. ago. This soil is overlain by Holocene eolian sand in which a very weak soil has developed.

Paleomagnetic analyses of the Fisher Valley sediments proved that interpretable polarity results could be obtained from these relatively coarse-grained, second-cycle red beds. The magnetic stratigraphy suggests that the basin fill was deposited during the time of the Brunhes, Matuyama, and Gauss Chronozones and, therefore, began to accumulate more than 2.5 m.y. ago. The sediments appear to contain a detrital remanent magnetization (DRM), carried mostly by specular hematite. The Matuyama reversed unit contains several intervals of normal polarity, which may correspond to normal events; however, the lack of detailed independent age control and evidence of post-depositional remagnetization in the reversed unit prevents positive identification of such polarity events.

The upper Cenozoic sediments in Fisher Valley have been extremely useful in deciphering the history of the Onion Creek diapir, whose upward movement impeded the flow of Fisher Creek, caused deposition and progressive deformation of the sediments in Fisher Valley, and finally diverted Fisher Creek away from the Colorado River into the Dolores River. The Fisher Valley sediments preserve the pattern and timing of this diapiric movement and provide a unique, detailed record of the history of one of the Paradox basin salt structures.

INTRODUCTION

Importance of the Upper Cenozoic Sediments in Fisher Valley

The upper Cenozoic sediments in Fisher Valley, southeastern Utah, constitute the best record of late Cenozoic conditions in the Paradox basin and perhaps in the entire Colorado Plateau province. Most of the Paradox basin and the Colorado Plateau province are characterized by erosional terrain and bare bedrock surfaces. Pliocene and Quaternary deposits in this area are highly local, thin, and discontinuous (Biggar and others, 1981). In contrast, Fisher Valley contains a sequence of Pliocene and Pleistocene deposits more than 145 m thick; these sediments record much of the late Cenozoic history of the area.

In addition to recording general late Cenozoic environments, the deposits in Fisher Valley have been gently, but complexly deformed by movement of the Onion Creek salt diapir (Colman, 1983). The young history of salt movement in the salt anticlines of the
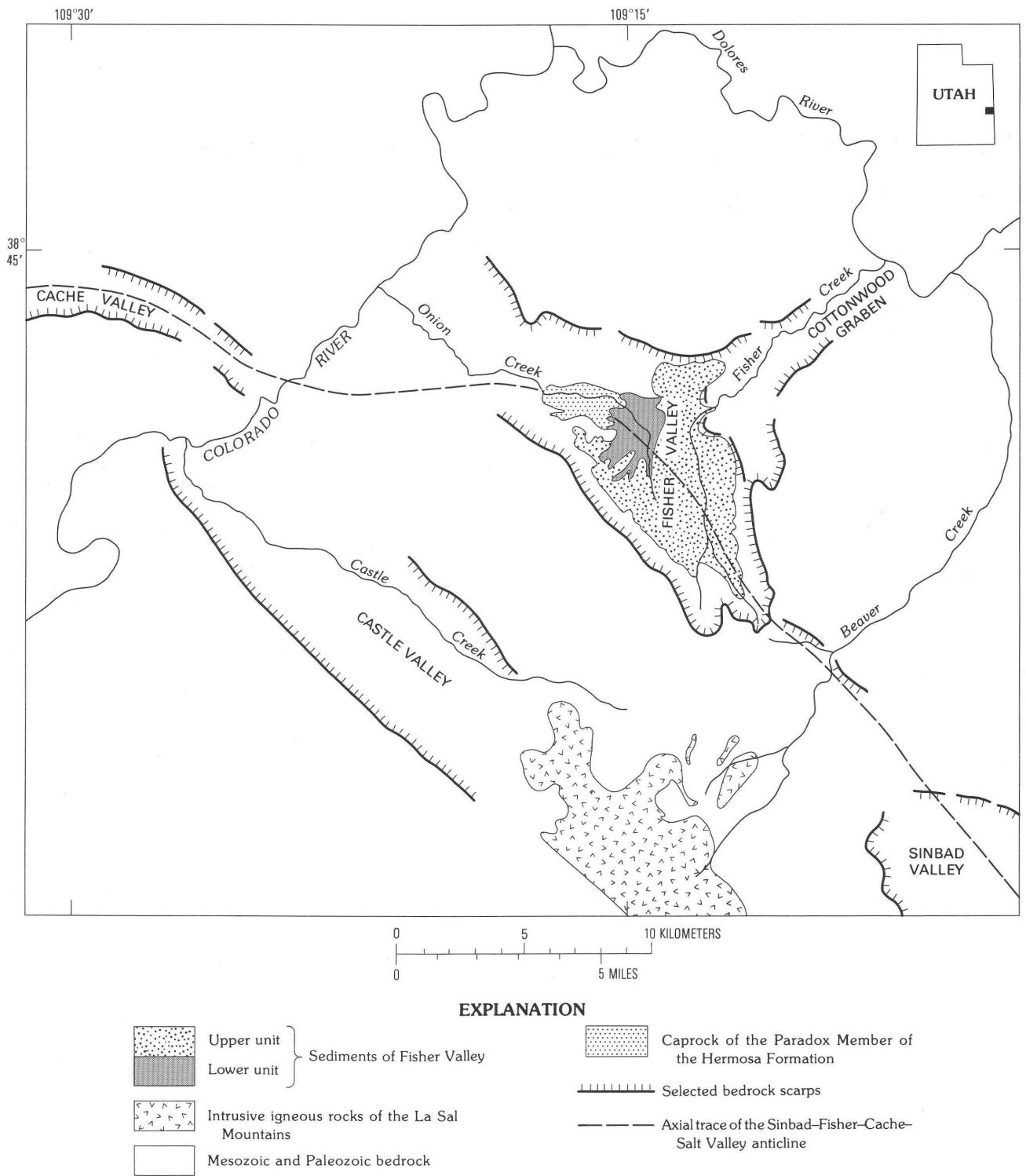
Figure 1. Location map of the Fisher Valley area, Utah. From Colman (1983).

EXPLANATION

Upper unit ⎫
           ⎬ Sediments of Fisher Valley
Lower unit ⎭

Intrusive igneous rocks of the La Sal Mountains

Mesozoic and Paleozoic bedrock

Caprock of the Paradox Member of the Hermosa Formation

⊥⊥⊥⊥⊥⊥⊥ Selected bedrock scarps

— — — Axial trace of the Sinbad–Fisher–Cache–Salt Valley anticline

Paradox basin is, in general, poorly known. The deposits in Fisher Valley are unique in that they allow detailed reconstruction of the late Cenozoic history of one of these salt bodies (Colman, 1983).

Previous Work

The upper Cenozoic deposits in Fisher Valley have received relatively little study, despite widespread interest

in the adjacent Onion Creek diapir. Dane (1935) described the Fisher Valley area in general terms in his reconnaissance work. Shoemaker (1954) mapped the detailed structures in the cap rock of the diapir and described deformation and unconformities in the adjacent upper Cenozoic deposits. Richmond (1962) described a section containing two volcanic ash beds in the Fisher Valley sediments. These two ash beds are now known to be the Lava Creek ash (0.61 m.y.) and the Bishop ash (0.73 m.y.) (Izett, 1981). Richmond also correlated some of the deposits in Fisher Valley with Quaternary deposits he mapped in and adjacent to the nearby La Sal Mountains.

Purpose

This report describes the detailed physical, soil, and paleomagnetic stratigraphy of the upper Cenozoic deposits in Fisher Valley. Together, these stratigraphic data form a time framework for reconstructing the late Cenozoic history of the Onion Creek salt diapir and for estimating environmental conditions in the Fisher Valley area during this time. The depositional history of the Fisher Valley area is the primary focus of this paper. The history of the Onion Creek salt diapir has been inferred from the deformation of the Fisher Valley sediments (Colman, 1983) and will be only briefly discussed here.

Acknowledgments

GEOLOGIC SETTING

Fisher Valley is located in the Paradox basin region of southeast Utah. The Paradox basin is delineated by the extent of salt within the Paradox Member (Middle Pennsylvanian) of the Middle and Upper Pennsylvanian Hermosa Formation. Salt and gypsum of the Paradox Member form the cores of the northwest-trending anticlines of the region. Repeated solution and flowage of salt within the Paradox Member have characterized the development of these salt anticlines since Pennsylvanian time (Cater, 1970).

The Fisher Valley salt anticline is part of a larger northwest-trending anticlinal structure that includes adjacent Cache and Sinbad Valleys (fig. 1) as well as Salt Valley to the northwest and Roc Creek Valley to the southeast. These valleys represent collapsed parts of structurally high sections along the crest of the anticline. The Onion Creek diapir, exposed in the collapsed crest of the Fisher Valley anticline, is essentially a cupola of salt emanating from the main diapiric core of the anticline. The cap rock of the diapir, along with a thick sequence of upper Cenozoic sediments, occupies the valley formed in the collapsed Fisher Valley anticline. The cap rock consists of the less soluble interbeds of the original evaporite sequence which, as a result of salt flowage and solution, are deformed into a chaotic jumble of gypsum, anhydrite, limestone, and shale. The sediments that are the subject of this report were deposited beginning in late Tertiary time, mostly in a basin east of the salt diapir. These basin-fill deposits consist of fluvial sand and gravel interbedded with lesser amounts of eolian silt and sand, all predominantly derived from Permian and Triassic formations that form the flanks of the Fisher Valley anticline.

The basin-fill deposits are in contact with the cap rock of the Onion Creek diapir and are exposed in an erosional amphitheatre that Onion Creek has cut into the sedimentary basin adjacent to the diapir (fig. 2). The sedimentary basin roughly corresponds to the area of the erosional amphitheatre and part of the area overlain by the perched floor of Fisher Valley (fig. 3). The upper Cenozoic deposits are more than 145 m thick and include the thickest Quaternary sequence in the Paradox basin and perhaps on the entire Colorado Plateau.

PHYSICAL STRATIGRAPHY

The upper Cenozoic deposits in Fisher Valley range from late Tertiary to Holocene in age (fig. 3). The basal unit is a Pliocene(?) or older gravel (unit Tg), which is complexly infolded into the cap rock of the Onion Creek diapir and is unconformably overlain by at least 145 m of Pliocene and Pleistocene basin fill. The basin-fill sediments (QTbl and Qbu) contain two volcanic ashes (fig. 4), at least nine buried soils, and along the basin margins at least four angular unconformities. The basin-fill deposits are capped by 1–5 m of Holocene eolian sand, which mantles the perched floor of Fisher Valley. A local unit of early Holocene alluvial sand (Qas of Colman and Hawkins, 1985), which apparently represents former valley-bottom deposits of Onion Creek, is inset into the basin-fill deposits near the eastern edge of the exposed diapir; it is about 30 m above the present channel of Onion Creek. Holocene alluvial deposits, 1–4 m thick, underlie channels and low terraces along Fisher and Onion Creeks. With the exception of the basal Pliocene(?)

Figure 2. Basin-fill deposits exposed in the erosional amphitheater at the head of Onion Creek. Oblique aerial view looking southeast; cultivated area is the perched floor of Fisher Valley. Cap rock of the Onion Creek salt diapir is the light-colored area in the foreground.

gravel, the deposits consist mostly of reddish-brown, very fine grained to coarse-grained sand and gravel derived from nearby red beds of the Permian Cutler and Triassic Moenkopi, Chinle, and Wingate Formations, which form the flanks of the Fisher Valley anticline. No macrofossils and only a few microfossils have been found in the Fisher Valley sediments, except in localized silt and sand of unit Qas.

Pliocene(?) Gravel

Pliocene(?) gravel (Tg), which underlies the basin-fill deposits (fig. 5), occurs in an isolated exposure along Onion Creek near the southeastern edge of the cap rock (fig. 3). The unit is as much as 25 m thick and consists of a fine, clast-supported gravel in a matrix of fine to coarse sand with distinct planar to cross bedding. The clasts are composed predominantly of intrusive igneous rocks derived from the La Sal Mountains and Mesozoic sedimentary rocks; more than 75 percent of the deposit

contains clasts of less than 10 cm in diameter. Similar deposits in nearby Castle Valley and in the Geyser and Roc Creek drainages have been assigned a Pliocene age, although the units have not been radiometrically dated (Cater, 1970; Carter and Gualtieri, 1965; Hunt, 1956). Paleomagnetic data, discussed in the Paleomagnetic Stratigraphy section, suggest that these deposits are more than 2.5 m.y. old.

Basin-fill Deposits

The basin-fill sediments are subdivided into a lower unit (QTbl) and an upper unit (Qbu). Along the margins of the depositional basin, these units are separated by an angular unconformity located at the base of the Lava Creek ash; toward the center of the basin, the lower and upper units become concordant. On the basis of the amount of secondary calcium carbonate and clay in buried paleosols (Soil Stratigraphy section) and the magnetic stratigraphy (Paleomagnetic Stratigraphy section)
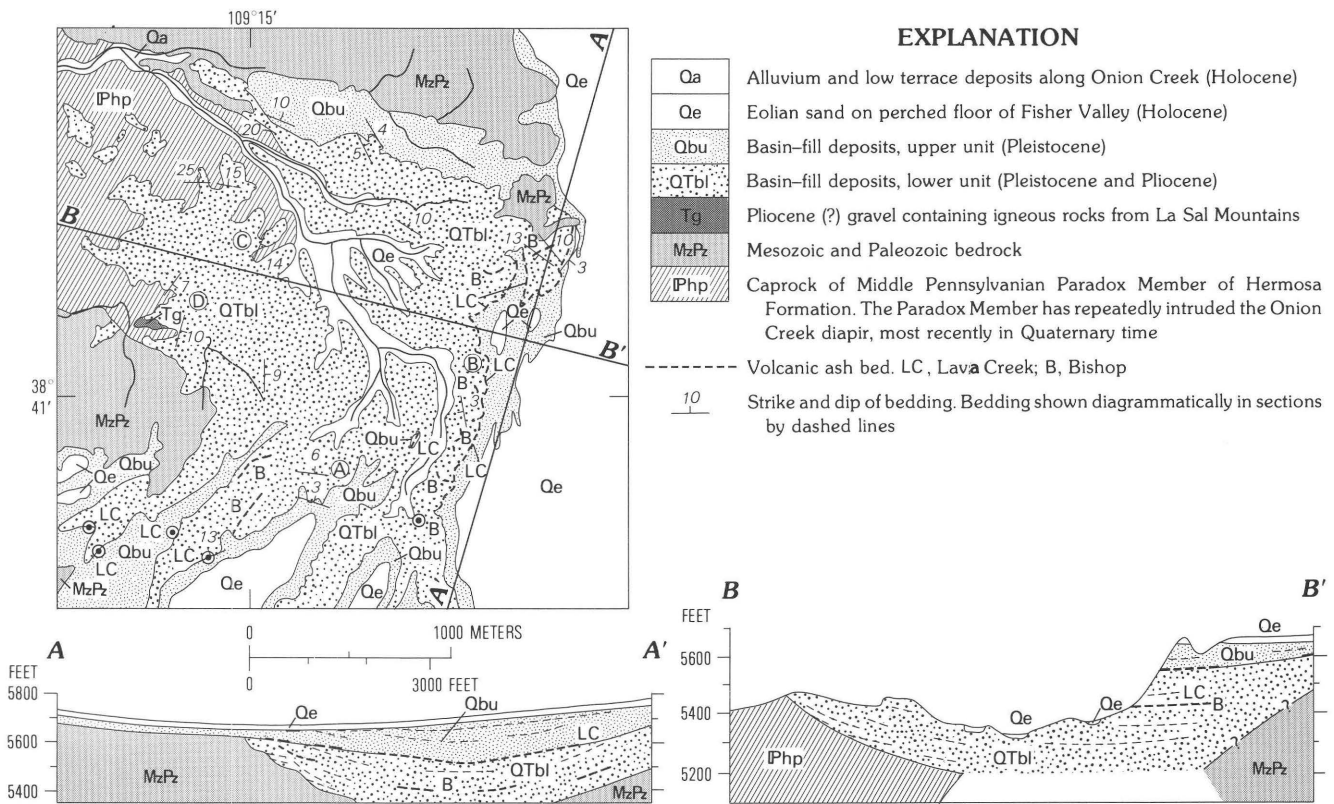
Figure 3. Geologic map and cross sections of the headwaters of Onion Creek, Fisher Valley, Utah. The nearby valley wall is projected into cross section A–A'. Circled letters represent the locations of sections shown in figure 6. From Colman (1983).

of the sediments, basin-fill deposition began before 2.5 m.y. ago and ended about 0.25 m.y. ago. The basin-fill deposits as a whole can be divided into nine or ten subunits that are separated by buried soils. Within each subunit, the deposits tend to form a crude pattern, beginning with fining-upward fluvial sand and gravel, grading into and overlain by massive eolian sand, in which a paleosol has developed. The subunits vary greatly in thickness, tending to be thicker in the lower part of the section; the paleosols also vary greatly in degree of development. Together, the depositional pattern and the soils suggest crude cycles of alternating sedimentation and
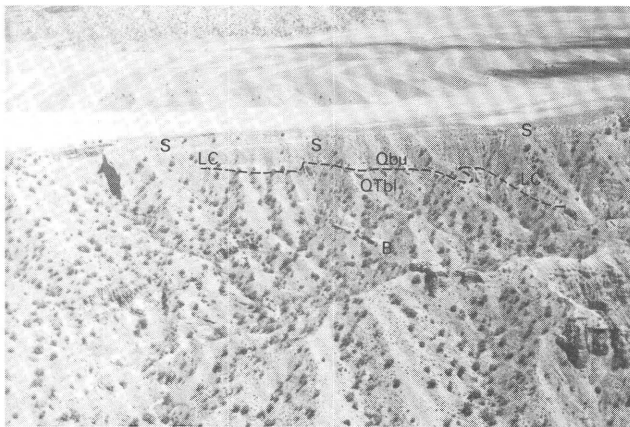
Figure 4. Lava Creek (LC) and Bishop (B) ashes. The ashes are interbedded with the upper and lower units of the basin-fill deposits (Qbu and QTbl, respectively). Light band (S) above Lava Creek ash is soil I. View to the east. From Colman (1983).
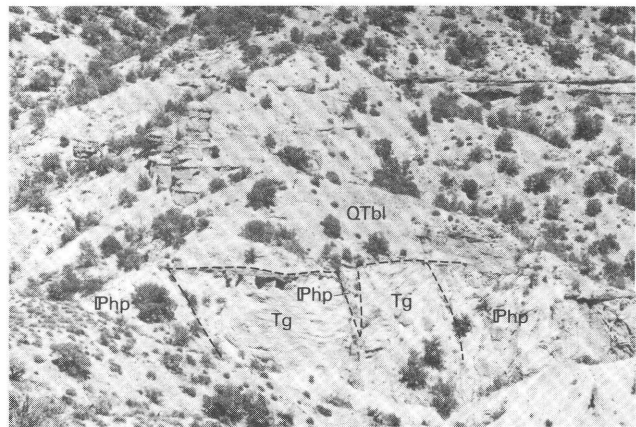
Figure 5. Deformed Pliocene(?) gravels (Tg). The gravels are folded into the cap rock of the Onion Creek diapir (Php) and are overlain by lower basin-fill deposits (QTbl). View to the north; trees are 2–3 m high. From Colman (1983).

landscape stability. Such cycles could be related to either climatic changes or to deformation of the Onion Creek diapir. Because the depositional subunits are more numerous than the pulses of diapiric uplift inferred from the deformation of the deposits and from unconformities (Colman, 1983), climatic change is probably at least partly responsible for the sedimentation-stability cycles.

The lower unit of the basin-fill deposits extends from the base of the Lava Creek ash to the Pliocene(?) gravel and is more than 100 m thick. Toward the center of the basin, this unit consists of moderately to strongly indurated, fine to coarse, calcareous sand interbedded with gravel. It includes three or four buried soils, two of which (soils A and C, fig. 6) are well developed. Much of the unit contains local cut-and-fill structures and cross-bedding; massive eolian sand composes the remainder. Toward the basin margins, the unit grades into predominantly matrix-supported gravel with minor lenses of medium to coarse sand; buried soils are not preserved near the basin margins. Minor angular unconformities occur in the unit near the edges of the basin. The Bishop ash occurs about 25 m below the top of a well-developed paleosol (soil C) that caps the unit (fig. 6). Buried soil A occurs about 40 m below the top of soil C and the base of the Lava Creek ash. Paleomagnetic data (Paleomagnetic Stratigraphy section) suggest that deposition of the lower unit began before 2.5 m.y. ago; soil data (Soil Stratigraphy section) and the position of the Lava Creek and Bishop ashes indicate that it ended shortly after 0.73 m.y. ago and well before 0.61 m.y. ago.

The upper basin-fill unit is as much as 50 m thick and, toward the center of the basin, consists predominantly of massive to medium-bedded, calcareous, moderately indurated sand with cut-and-fill structures and minor lenses of fine to medium gravel. The Lava Creek ash locally occurs at the base of the unit and is as much as a meter thick. Where the Lava Creek ash is absent, the basal few meters of the unit tend to be thinly bedded to laminated and ash-rich. The unit contains at least six buried soils (soil D to soil I, fig. 6) and, near the basin margin, at least one angular unconformity. Toward the edges of the basin, the unit thins and consists predominantly of moderately indurated, matrix-supported gravel with clasts as much as 1.5 m in diameter. A well-developed, buried calcic soil (soil I, fig. 6) caps the upper unit. Long-term rates of secondary carbonate accumulation (Soil Stratigraphy section) suggest that this soil began to form about 0.26 m.y. ago. In addition, uranium-trend analyses of the soil suggest an age of about 0.21 m.y. for the upper (0–1 m) part of the parent material and 0.24 m.y. for the lower (1–3 m) part (J. N. Rosholt, Jr., written commun., 1983). Therefore, the upper unit of basin fill, which extends from the Lava Creek ash to soil I, was deposited between about 0.61 and 0.25 m.y. ago.

Holocene Deposits

A unit of unstratified, reddish-brown eolian sand and silt (Qe), 1–5 m thick, overlies soil I (fig. 6) and the upper unit of the basin-fill deposits. The eolian sand mantles the perched floor of Fisher Valley (fig. 3) and forms small dunes at the edge of the bluffs near the headwaters of Onion Creek. A very weak soil (soil J, fig. 6) has developed in the upper part of the eolian sand; the poor development of this soil and the preservation of dune morphology suggest a Holocene age for unit Qe.

A localized unit of yellow to gray, nonindurated, calcareous silt and fine to coarse sand (Qas of Colman and Hawkins, 1985; area too small to be shown in fig. 3) unconformably overlies the lower unit of basin fill near the eastern edge of the cap rock. The sediments are inset into the basin-fill deposits and are as much as 30 m above the present channel of Onion Creek. They are as much as 10 m thick and contain laminated beds with layers of peaty material 1–2 cm thick. A radiocarbon age of 9330 ± 155 yr (DIC–2527) was obtained from peaty sand near the middle of the unit. These sediments also contain a fauna consisting of abundant ostracodes and terrestrial gastropods along with rare bivalves and aquatic gastropods. The faunal assemblage suggests that the sediments were deposited in a marshy environment whose water was derived from nearby, relatively fresh springs (R. M. Forester, written commun., 1983). Similar or slightly drier conditions now exist on the valley bottom in the erosional amphitheater at the headwaters of Onion Creek; unit Qas appears to represent material deposited on the former valley floor of Onion Creek, which was cut into the basin-fill sediments about 9,000–10,000 yr ago.

Holocene alluvium, 1–4 m thick, underlies channels and low terraces along Fisher and Onion Creeks (unit Qa in fig. 3 and in Colman and Hawkins, 1985). The alluvium consists of nonindurated to slightly indurated, coarse calcareous sand and contains variable amounts of subangular to subrounded gravel. A very weak soil occurs in the upper part of the low terraces. Charcoal from these terraces yielded radiocarbon dates that are modern within analytical error (DIC–2525, 2536, 2537, 2538).

SOIL STRATIGRAPHY

Introduction

Buried and surface soils are an important part of the stratigraphy of the upper Cenozoic deposits in the Fisher Valley area. These soils mark hiatuses in the deposition of the basin-fill sediments in Fisher Valley and reflect times of relative landscape stability in the area.
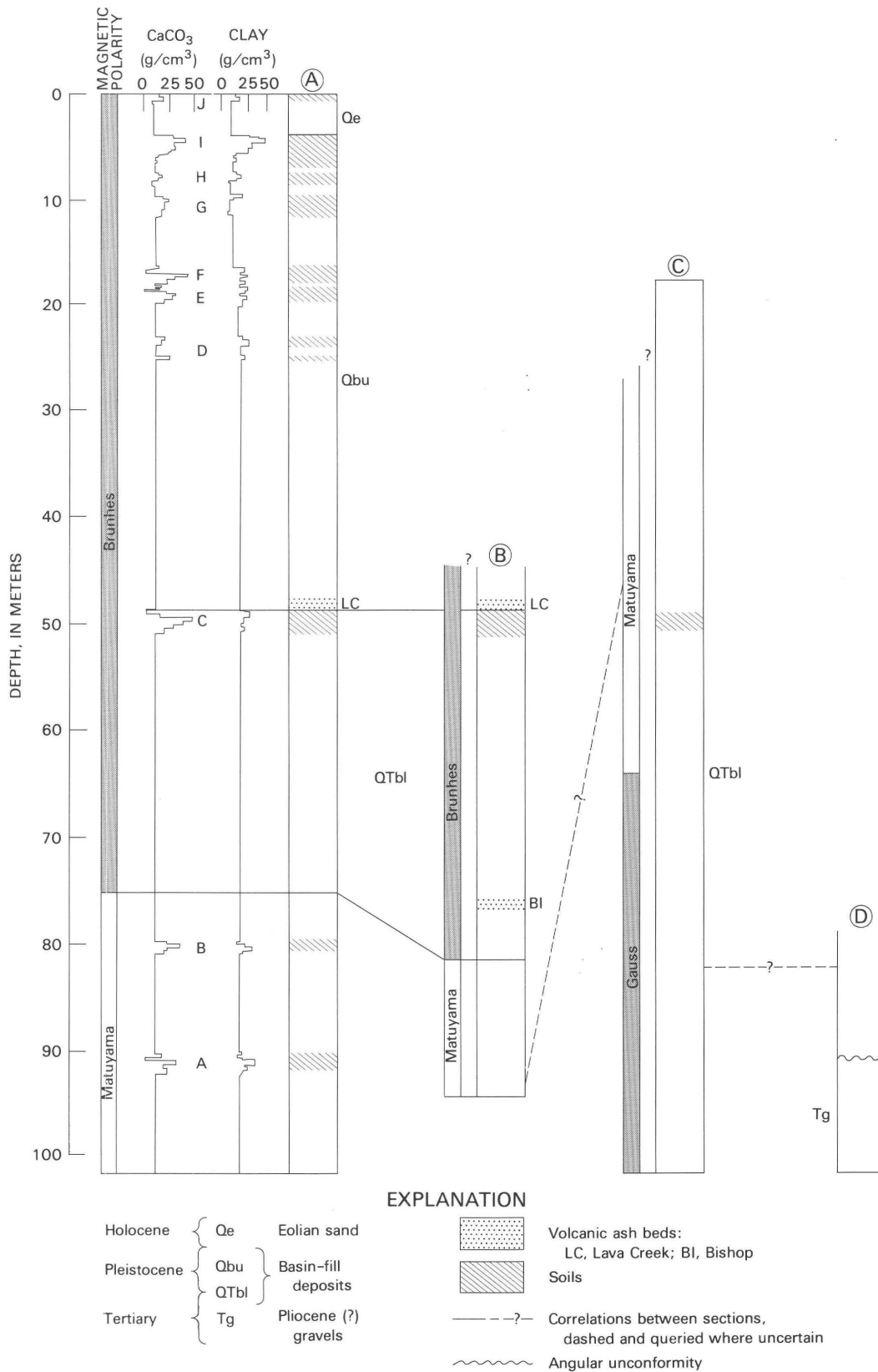
Figure 6. Stratigraphic sections of the basin-fill deposits. In the magnetic polarity column, solid is normal and open is reversed. Circled letters above columns are stratigraphic sections referred to in the text; locations are shown in figure 3. Sections are correlated by stratigraphic markers and by mapping of limited continuous exposures.

In addition, the secondary clay and calcium carbonate contents of the soils are useful for estimating ages. As discussed in the section on physical stratigraphy, the soils mark the latter part of crude sedimentary cycles, in which deposition of fluvial sand and gravel is followed by deposition of massive eolian sand, in turn followed by soil formation. The buried soils are interspersed throughout the basinfill deposits; they are relatively rare in the lower part and become increasingly common in the upper part (figs. 6 and 7). The most strongly developed soil in the sequence occurs at the top of these deposits and marks the end of basin-fill deposition.

Parent materials for the soils were derived from Paleozoic and Mesozoic red beds that surround the area. Most of the soils described here are developed in relatively fine grained, reddish-brown, calcareous eolian sand, which is locally interbedded with stratified fluvial sand and gravel derived from the same bedrock units. Near the edges of the late Cenozoic depositional basin, gravel becomes increasingly common, and many of the soils are eroded or truncated. In addition, multiple soils in the center of the basin merge into single soils because of nondeposition near the basin margins.
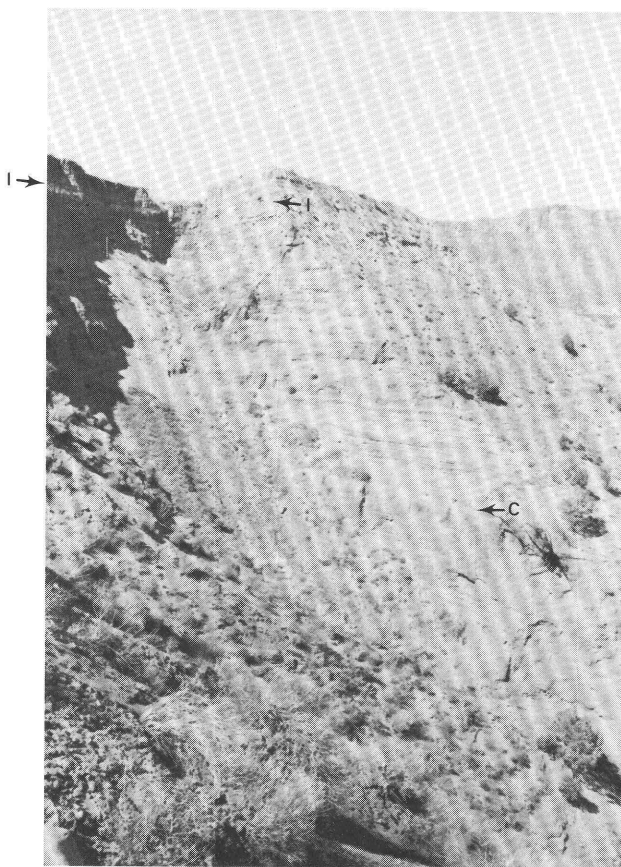
Figure 7. Buried soils intercalated with basin-fill deposits in landslide scarp. Arrows indicate two prominent buried soils (soils I and C). Five less prominent buried soils occur between soils I and C, which are about 45 m apart vertically.

Most of the buried soils in the section are more strongly developed than Holocene soils in the area. Under present conditions, B horizons are minimal, most soils are calcareous throughout, and degree of soil development is expressed primarily as calcareous C-horizon properties. In contrast, the buried soils in the basin-fill deposits in Fisher Valley have leached, relatively well developed B horizons and C horizons more strongly developed than those of Holocene soils.

Many of the soils developed in the basin-fill sediments appear to be polygenetic, that is they formed under varying climatic conditions. The buried soils commonly show concentrations of secondary carbonate at more than one depth in the soil. The shallower zones are inferred to have been superimposed during more arid conditions on more deeply leached B horizons formed during relatively moist conditions. The most strongly developed soil (soil I), at the top of the basin-fill deposits, most clearly shows polygenetic properties (fig. 8).

The soils that will be discussed here are those developed in the upper (Qbu) and lower (QTbl) basin-fill units of Colman and Hawkins (1985) and the soil in the overlying Holocene eolian sand. Soils in other surficial units in the Fisher Valley area are either eroded or are developed in deposits so young that soil development is minor. The climate of the Fisher Valley area is semiarid; climatic records for Gateway, Colo., and Moab, Utah (U.S. Dept. of Commerce, 1953; National Oceanic and Atmospheric Administration, 1981), suggest that for the Fisher Valley area, the mean annual temperature is about 12 °C (range of monthly averages about –2 to 25 °C), and the mean annual precipitation is about 25 cm (range of monthly averages about 1.3–3.0 cm).

Data and Methods

Both field and laboratory data were collected for the soils developed in the basin-fill deposits in Fisher Valley (appendix, table 4). Field data consist of profile descriptions, including horizon identification, depth, Munsell color, texture, ped structure, and calcium carbonate morphology. Channel samples of each horizon were taken, and grain size, carbonate content, bulk density, and weight-loss-on-ignition were analyzed in the laboratory. Grain-size analyses were performed by sieve and pipette methods, carbonate content was determined by the Chittick gaseometric carbonate-dissolution technique (Dreimanis, 1962), and bulk density was measured by the water dispacement method on ovendried, paraffin-coated ped samples (Chleborad and others, 1975). Soil-horizon nomenclature follows that of Birkeland (1984) and Guthrie and Witty (1982).
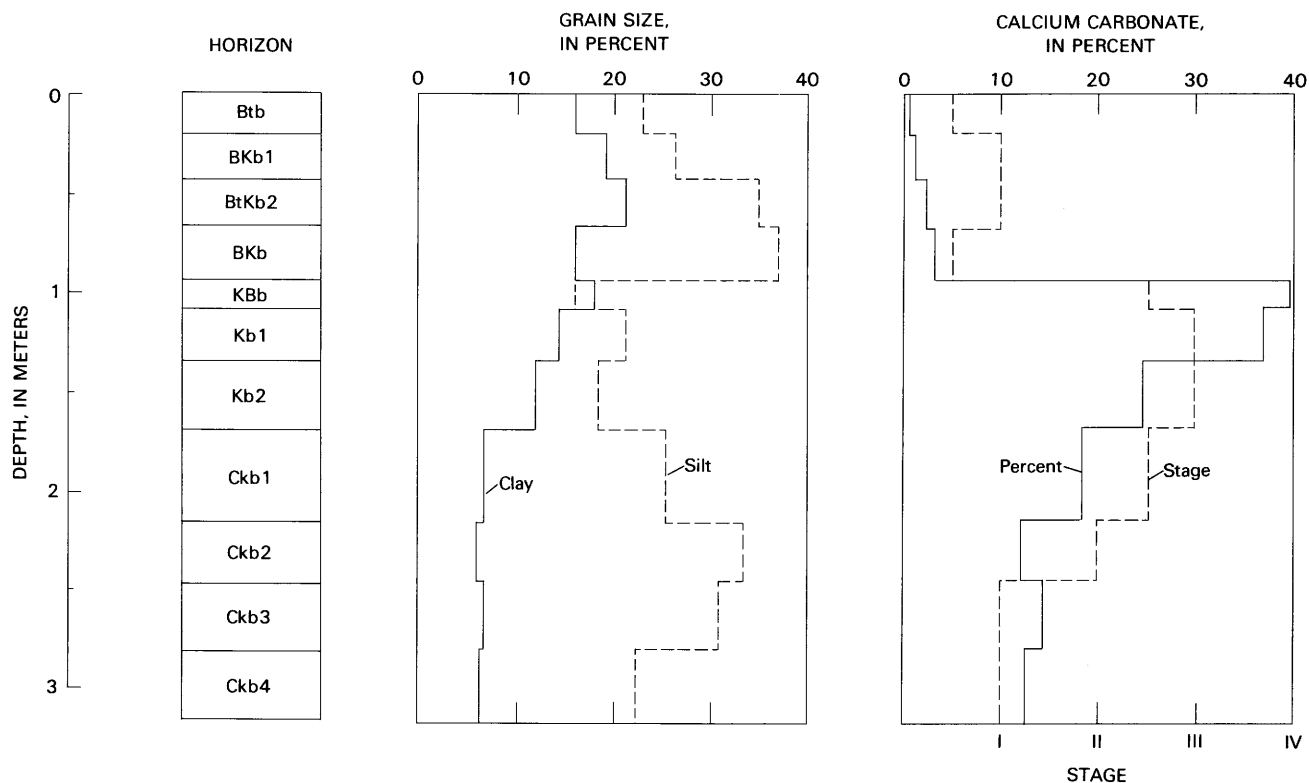
Figure 8. Grain size and calcium carbonate data for soil I. Data from table 4, appendix.

Rates of Soil Formation and Ages

Soils in the Fisher Valley area provide stratigraphic and age information for the upper Cenozoic basin-fill deposits. In addition to the stratigraphic position of the soils, their degree of development and their rates of formation are of major concern. Recent studies of the degree of development and the rates of formation of arid-climate soils (Harden and others, 1985; Machette, 1985) show that progressive and systematic changes in soil development occur with time. Key soil properties that show these changes are the morphology and amounts of secondary calcium carbonate and clay. Quantitative measurements of these properties are especially useful in estimating soil ages and long-term accumulation rates.

Secondary Calcium Carbonate

Processes and rates of formation of calcic soils have been rather controversial. Calcic soils are characteristic of most of the arid and semi-arid regions of the western United States, but they have commonly been confused with other types of carbonate accumulation. However, recent work on calcic soils has resulted in better definitions of calcic soils, better descriptions of their morphology and other characteristics, and better understanding of the processes by which they form. (See Gile and others

(1981) and Machette (1985) for summaries.) In addition, considerable data have been collected on the rates of formation of calcic soils and on variation in these rates with climate and carbonate source.

Calcic soils are generally considered to form primarily by redistribution of (1) the original carbonate in soil parent materials and (2) secondary carbonate added to the soils from precipitation, either in the form of solid aerosols or as dissolved calcium carbonate (Gile and Grossman, 1979; Gile and others, 1981; Machette, 1985). Other sources of calcium, such as the weathering of calcium-rich rocks and precipitation from calcium-rich capillary fringe of shallow ground water, are thought to be negligible sources of Ca^{2+} (Machette, 1985). Parent materials of the soils in the Fisher Valley area are mostly quartz-rich sand derived from Paleozoic and Mesozoic red-bed sandstones; those parent materials contain significant amounts of primary $CaCO_3$ derived from the cement of the sandstone bedrock, but little or no other source of Ca^{2+}.

Because secondary carbonate accumulates in calcic soils in a systematic way with time (Gile and others, 1981; Machette, 1985), the amount of secondary carbonate in a soil can be used to estimate the duration of soil formation. Durations of soil formation, in turn, can be used to estimate ages of deposits in a stratigraphic section. We have used secondary carbonate to estimate the ages of the deposits in Fisher Valley, essentially following the

methods of Machette (1978, 1985). These methods use long-term average rates of secondary carbonate accumulation to estimate durations of soil development.

Total secondary carbonate in the soil (cS) (Machette, 1985) is defined as the sum of the secondary carbonate in each of the soil horizons (cs) where

$$cs = (c_3P_3 - c_1P_1) \, d$$

and c_3 is the present weight percent carbonate, c_1 is the original weight percent carbonate, P_3 is the present bulk density, P_1 is the original bulk density, and d is the horizon thickness. Original carbonate percentages and bulk densities were estimated from the lowermost, least altered C horizons of the soils (appendix, table 4) and from several samples of sediment that were not in soils. For gravelly parent materials, the calculations were made separately for the gravel (>2 mm) and for the sand and finer fractions (<2 mm), and total secondary carbonate values were corrected for the volume of the soil occupied by the gravel. All calculations of secondary carbonate for the soils in Fisher Valley are given in table 5 in the appendix.

Ages for the vertical sequence of soils and sediments were estimated by methods analogous to those used by Machette (1978). Total secondary carbonate values (cS) were summed from all the soils above stratigraphic datums of known age. The Lava Creek ash (0.61 m.y.; Izett, 1981) and the Brunhes/Matuyama paleomagnetic boundary (0.73 m.y.; Mankinen and Dalrymple, 1979) were used as time datums. The total secondary carbonate above a time datum divided by the age of the datum gives an estimate of the long-term average rate of carbonate accumulation, and this rate is used to calculate the time required to accumulate the secondary carbonate in each soil (table 1). Results based on the two datums are nearly identical; the calculations using only one datum (the Brunhes/Matuyama boundary) are shown in table 1.

This method of estimating ages from the secondary carbonate content of soils in a stratigraphic section requires several critical assumptions. First, the time represented by soil formation is assumed to be related to the time necessary for sediment deposition: either (1) soil formation takes up virtually all the time represented by the stratigraphic section, which is contradicted by the paleomagnetic results, or (2) the time required for soil formation is a constant proportion of the time represented by each sediment-soil unit. This assumption is convenient as a first approximation for fluvial and eolian sediments, but is difficult to evaluate except in terms of empirical results.

The second major assumption is that the long-term rate of secondary carbonate accumulation is constant. Because of climatic controls on moisture and rates of aerosolic influx, short-term rates of carbonate accumulation clearly vary. The difference between carbonate accumulation rates for Holocene time compared to late Pleistocene time may be as much as a factor of two or more (Machette, 1985). However, because climate for about the last 1 m.y. has fluctuated around a nearly constant mean value with an overall periodicity of about 100,000 yr (Hays and others, 1976), and because Holocene and late Pleistocene conditions represent climatic extremes, periods of more than about 50,000 yr may represent a nearly constant long-term average (Machette, 1985).

Ages derived from long-term average rates of carbonate accumulation for the parent materials of soils in

Table 1. Ages of soils estimated from secondary calcium carbonate and clay contents

Soil	Secondary carbonate			Secondary clay		
	Amount (g/cm²)	Duration[1] (10³ yr)	Period[1] (10³ yr)	Amount (g/cm²)	Duration[2] (10³ yr)	Period[2] (10³ yr)
J	0.8	5	0–5	2.7	24	0–24
I	39.8	257	5–262	35.9	318	24–342
H	12.1	78	262–340	9.0	80	342–422
G	8.1	52	340–392	3.3	29	422–451
F	13.0	84	392–476	6.8	60	451–511
E	13.2	85	476–561	14.4	127	511–638
D	5.5	35	561–596	0.0	0	0
			— Lava Creek ash, 610,000 yr —			
C	20.5	132	596–730	10.2	90	638–730
			— Brunhes/Matuyama boundary, 730,000 yr —			
B	9.4	61	730–791	6.6	58	730–788
A	8.2	50	791–841	14.9	132	788–920

[1]Calculated from an average accumulation rate of 0.15 g/cm²/10³ yr, derived from the cumulative amount of secondary carbonate (113 g/cm²) above the Brunhes/Matuyama boundary.

[2]Calculated from an average accumulation rate of 0.11 g/cm²/10³ yr, derived from the cumulative amount of secondary clay (81 g/cm²) above the Brunhes/Matuyama boundary.

the Fisher Valley sediments (table 1) seem reasonable compared to what little is independently known about their ages. First, use of either the Lava Creek ash (0.61 m.y.) or the Brunhes/Matuyama paleomagnetic boundary (0.73 m.y.) as a time datum yields nearly identical long-term average rates of secondary carbonate accumulation, about 0.15 g/cm^2/10^3 yr. This rate compares favorably with the rate of 0.14 g/cm^2/10^3 yr for the Beaver area in south-central Utah (Machette, 1985), and with the maximum rate of 0.14–0.26 g/cm^2/10^3 yr for Spanish Valley (Harden and others, 1985), located about 27 km southwest of Fisher Valley. Second, carbonate accumulation rates for Fisher Valley suggest an age of about 260,000 yr for the parent material of soil I, the soil that caps the basin-fill deposits in Fisher Valley. This age compares favorably with ages of 210,000 and 240,000 yr for the upper and lower parts, respectively, of the sediments in which soil I is formed (J. R. Rosholt, written commun., 1983), as determined by uranium-trend methods (Rosholt, 1985).

Secondary Clay

Clay content of soils, especially secondary clay, is a useful index of soil development. Total and secondary clay contents are commonly used as an indicator of age (Birkeland, 1984), but in few cases has clay content been quantitatively used to estimate numerical soil ages (Pierce, 1979; Levine and Ciolkosz, 1983). In many respects, the accumulation of secondary clay is analogous to the accumulation of secondary carbonate and can be treated in a similar manner to estimate ages. However, the use of secondary clay to estimate soil ages involves several problems in addition to those encountered in using secondary carbonate for this purpose: (1) in many environments, weathering processes produce clay-size material in soils, in addition to that produced from other sources; (2) the original clay content of many parent materials is more variable and more stratified than is their carbonate content; and (3) B horizons are more prone to erosion than C horizons.

Conditions in the Fisher Valley area are not conducive for clay formation by weathering. The climate is semiarid, and the parent materials contain high percentages of resistant quartz sand. Therefore, secondary clay derived from in-situ weathering is probably negligible. The primary sources of clay in the Fisher Valley soils are the original clay content of their parent materials and clay derived from aerosolic sources (dust and precipitation nucleii), the same sources that are dominant for secondary carbonate. Thus, secondary clay can be used in the same way that secondary carbonate was used to estimate ages, with additional uncertainty related to variable parent materials and erosion.

Total secondary clay in a soil column (g/cm^2) was calculated by methods similar to those used to calculate secondary carbonate (appendix, table 6). The calculations are somewhat simpler than those for carbonate, because the gravel fraction of the soils does not contain or contribute any secondary clay. Clay contents were corrected for the volume of the soil occupied by gravel.

Ages for soil parent materials were calculated from secondary clay (table 1) by the same methods and with the same assumptions that were used for secondary carbonate. Long-term average rates of accumulation were calculated from the total amount of secondary clay above the time datum of the Brunhes/Matuyama boundary. The long-term rate was then used to calculate ages for the soils from the amount of secondary clay in each soil, assuming a constant proportion of time for sedimentation and a constant clay-accumulation rate. The arguments for the validity of these assumptions are the same as those presented for the age calculations made using secondary carbonate.

The ages derived from secondary clay contents are consistently older, and probably less reasonable, than those derived from secondary carbonate contents. The age calculated for the parent material of soil J is 24,000 yr, which is too old relative to geologic relations that suggest a Holocene age for the parent material. An age of 318,000 yr was calculated from secondary clay contents for soil I, which is considerably older than the uranium-trend ages (210,000 and 240,000 yr) discussed in the Physical Stratigraphy section. Because the original clay contents of the soils are difficult to estimate due to variability and stratification in the parent material, the amount of secondary clay in soils I and J may have been overestimated. However, similar long-term average rates of secondary clay accumulation are derived whether the Lava Creek ash or the Brunhes/Matuyama boundary is used as a time datum, about 0.11 g/cm^2/10^3 yr, which support the general validity of the method.

Summary

Secondary carbonate and clay contents provide a quantitative method of measuring soil development in the Fisher Valley sediments. These data in turn provide stratigraphic and time information for the sequence. For Fisher Valley, as for other semiarid and arid areas, the main sources of clay and carbonate in the soils seem to be aerosolic inputs and the original content of these materials in the sediments; contribution of carbonate and clay from weathering or other sources appears to be negligible. Long-term rates of accumulation of both carbonate and clay appear to be nearly constant for intervals of 10^5 yr or more.

The primary source of error in using carbonate- and clay-accumulation rates to calculate soil ages comes from

SECTION A

SECTION B

LAVA CREEK ASH

0

50

POLARITY
CHRONOZONE

SECTION C

60

BRUNHES

0.73 m.y.

BISHOP ASH

70

80

?

90

MATUYAMA

?

?

?

100

EXPLANATION

□   Cube
◇   Cylinder
○   Core
■   Normal
⊠   Normal (?)
□   Reversed
⊠   Reversed (?)
◧   Indeterminate
∿   Unconformity
⌇⌇⌇   Paleosol
∞∞∞   Volcanic ash

110

2.48 m.y.

GAUSS

120

DEPTH, IN METERS

130
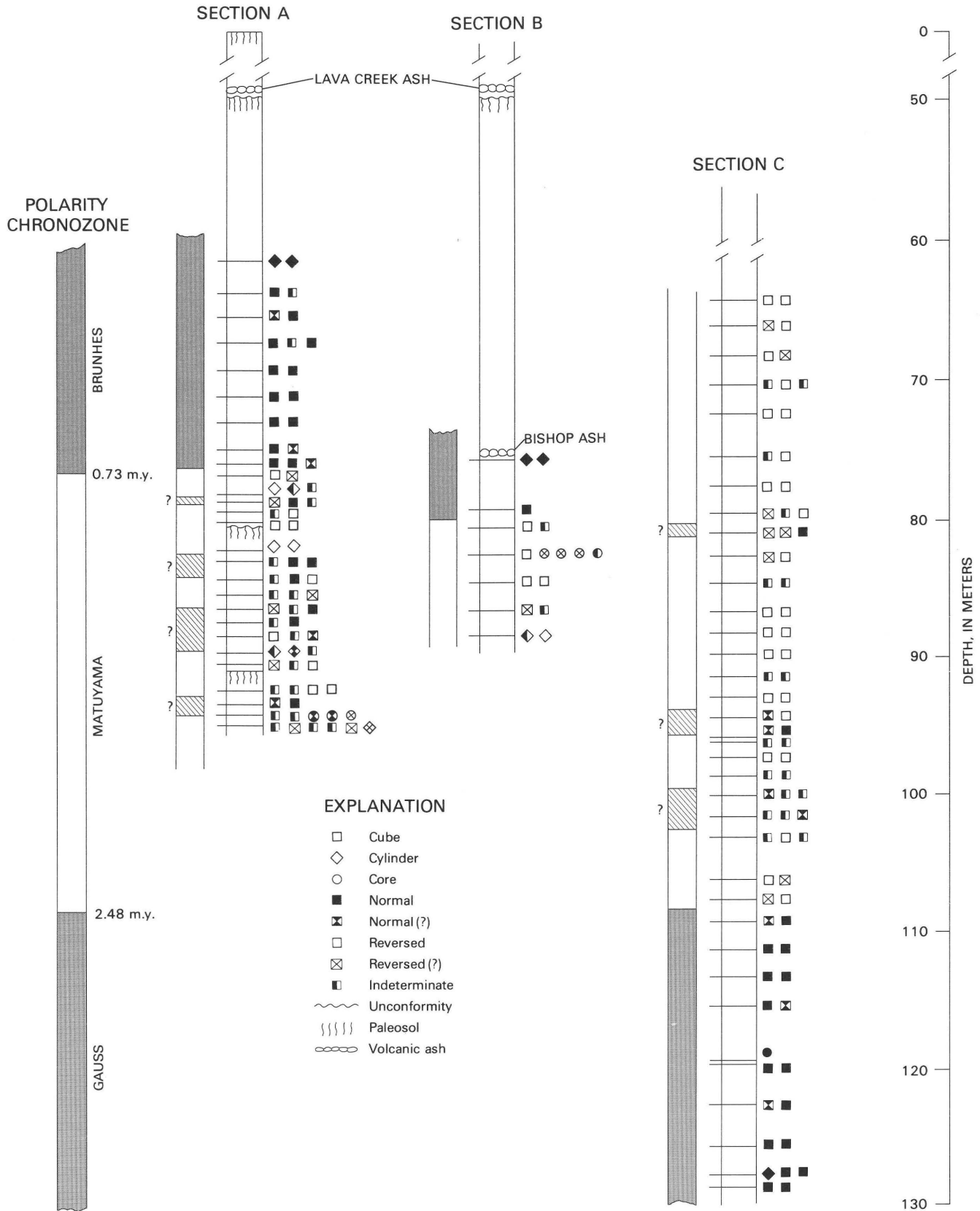
difficulties in estimating the original carbonate and clay contents of the parent materials; this problem seems more serious for clay than for carbonate. Rates of carbonate accumulation produce ages that seem more reasonable than those derived from rates of clay accumulation. The long-term rate of carbonate accumulation at Fisher Valley (about 0.15 $g/cm^2/10^3$ yr) is similar to rates calculated for nearby areas and yields ages that are consistent with independent age control.

PALEOMAGNETIC STRATIGRAPHY

Introduction

The basin-fill deposits in Fisher Valley contain few materials from which the age of the sediments can be estimated. The Lava Creek and Bishop ashes and several paleosols provide age control for the upper part of the stratigraphic section, but the lower part of the section, below the Bishop ash, contains very few datable materials. Consequently, paleomagnetic stratigraphy provided the primary information about the age of these sediments.

Although coarse-grained, second-cycle red sediments, such as those in Fisher Valley, are generally thought to be poor recorders of paleomagnetic directions, preliminary samples and analyses indicated that the deposits contained a credible paleomagnetic record. Where stable sediments (paleosols and volcanic ash beds) occurred in the section, the observed paleomagnetic record was consistent with the polarities in the standard paleomagnetic time scale (Mankinen and Dalrymple, 1979), and adjacent samples yielded reasonably consistent polarities. After further sampling throughout the part of the stratigraphic section below the Lava Creek ash (QTbl in fig. 6), we were able to define the paleomagnetic stratigraphy. Ages of the volcanic ash deposits and the buried soils in the upper part of these sediments in conjunction with the magnetic reversal stratigraphy in the section were thus used to investigate the timing of remanence acquisition and to correlate polarity zonation in the sediments with the standard magnetic-polarity time scale to determine the timing of deposition (Choquette and Colman, 1983).

Sampling

We collected oriented samples from three stratigraphic sections exposed in the headwaters of Onion Creek. The sampled sections, A, B, and C (fig. 3), are 35, 15, and 65 m thick, respectively. A total of 168 samples were collected at 1- to 2-m intervals from 70 horizons in the sections (fig. 9). Two or more samples were collected from most of these horizons.

Three techniques were used to obtain samples both from oriented hand specimens in the laboratory and from undisturbed exposures in the field. Most of the samples (146) were collected by carving cubes from planed surfaces in the sediments. The cubes were then placed in plastic sample boxes. Fourteen samples were obtained by pushing thin-walled plastic cylinders into the sediments. The cylinders and boxes were sealed with either plastic lacquer or acetate cement. Eight samples were drilled with a diamond core bit. The cubes, cylinders, and drill cores have volumes of 3.2, 6.5, and 10.9 cm^3, respectively. We used a Brunton compass to orient all samples in the field with an estimated accuracy of $\pm 5°$.

Sampling was conducted in several phases. Initially, we collected a set of samples at widely spaced intervals to determine the stability of magnetic remanence upon demagnetization and the polarities of sediments in the composite section. Subsequent samples were collected at more closely spaced intervals to locate polarity boundaries and to substantiate polarities in previously sampled horizons.

Paleomagnetic Remanence

Remanence Measurement

Remanent magnetization was measured in a digital spinner magnetometer with a sensitivity of about 5×10^{-4} A/m (amperes/meter). Remanent directions for samples collected from tilted beds (maximum dip, 14°) were corrected for bedding attitudes.

The core samples were thermally demagnetized in steps of 100° to 200°C at temperatures ranging from 100 to 680°C. The samples from plastic cubes and cylinders were demagnetized in a three-axis tumbler at peak alternating fields (AF) of 10, 20, 40, and 60 mT (millliteslas). Peak AF intermediate to or exceeding these levels were

---

Figure 9 (facing page). Composite paleomagnetic stratigraphy in the basin-fill deposits. Sample polarities are shown to the right of the stratigraphic sections. Queried intervals in the Matuyama Polarity Chronozone denote subzones containing normal polarities. These subzones may correspond to normal polarity subchronozones and (or) post-depositional magnetic overprinting of the sediments. Polarity time scale from Mankinen and Dalrymple (1979).

applied to samples showing unstable directions or large intensity changes at low levels of demagnetization and to those failing to reach stable directions by 60 mT.

Polarity Classification Scheme

Each sample was assigned one of the following polarity classes: normal, normal(?), reversed, reversed(?), or indeterminate (N, N?, R, R?, I, respectively). Each of these classes is represented by a region of an equal-area projection (fig. 10).

The limits for N and R polarity are based on estimated limits of secular variation and inclination error. Any direction within 30°, the estimated limit of secular variation (Channel, 1982), of the normal (reversed)

EXPLANATION

———	Projection to lower hemisphere (positive inclination)
– – –	Projection to upper hemisphere (negative inclination)
◓	Normal Polarity
◔	Reversed Polarity
○	Normal (?) Polarity
◌	Reversed (?) Polarity
◍	Indeterminate Polarity
●	Expected mean dipole directions
○	

Figure 10. Equal-area projection showing polarity classes of single-component paleomagnetic samples. Limits of N and R polarities (stippled) are based on estimated secular variation and inclination error. Limits of N(?) and R(?) polarities are 60 angular degrees from the expected dipole field at the sampling locality.

axial dipole field was assumed to be N (R). However, depositional remanent magnetism may be subject to a variety of errors including inclination error, current-rotation error, and bedding error (Verosub, 1977); and laboratory tests suggest that these errors can be significant (King, 1955; Griffiths and others, 1957; Rees, 1961). Although it is difficult to evaluate the actual influence of such errors in the Fisher Valley deposits, we decided to expand the limits of the N (R) region by applying an empirical function for inclination error to the boundary defined by secular variation. We used the empirical function developed by Griffiths and others (1960) and allowed for a maximum inclination error of 30°, which occurs for an ambient field inclination of 58°. The resulting boundary is shown in figure 10. We arbitrarily set the limit of N? (R?) polarities at 60 angular degrees from the normal (reversed) axial dipole direction. These polarity limits allow considerable variation in magnetic remanence, but they seem reasonable considering the directional scatter that can result from post-depositional compaction and mechanical forces accompanying deposition of coarse-grained sediments (Verosub, 1977).

Samples that contained a single magnetic component (fig. 11A) were classed according to the regions shown in figure 10. Most of these samples showed consistent directions at demagnetization levels exceeding 20 mT or 300 °C. However, some samples yielded stable directions during low levels of demagnetization but showed large directional changes and fluctuating magnetic intensities after demagnetization at AF exceeding about 40 mT. This behavior was attributed to anhysteritic remanent magnetization (ARM) acquired during AF treatment, and the polarity of such samples was determined from directions measured at low AF treatment.

Samples that contained multiple magnetic components were classified on the basis of orthogonal projections of remanent vectors (Zijderveld, 1967). Samples were classed N? or R? when the plots revealed N, N?, R, or R? components that remained stable for at least three consecutive levels of demagnetization (fig. 12). All other samples that showed either consistent I directions or unstable directions upon demagnetization were classed I (fig. 11B).

Stepwise Demagnetization

Magnetic intensity of the paleomagnetic samples ranged from 0.3 to 24.8×10^{-3} A/m. The geometric mean natural remanent magnetization (NRM) intensity of all samples was 2.2×10^{-3} A/m. Magnetic intensities differed considerably between normal- and reversed-polarity zones and between sample polarity classes (table 2). Mean NRM intensity of reversed-polarity samples was consistently lower than that of normal-polarity samples.
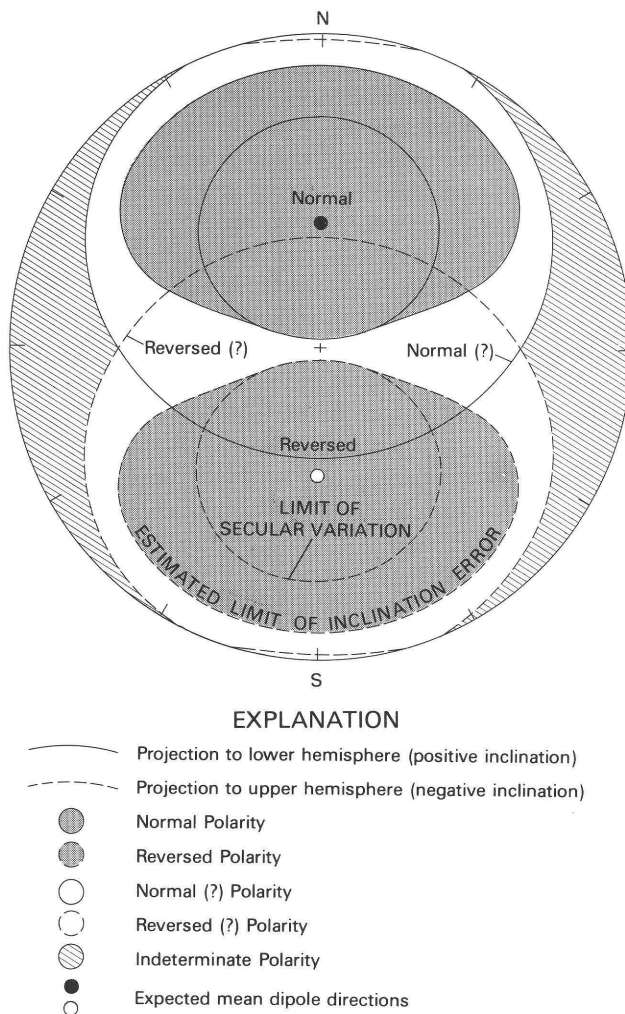
EXPLANATION

•   Lower hemisphere projection

○   Upper hemisphere projection

•60   Level of stepwise demagnetization, in milliteslas

①   Sample reference number
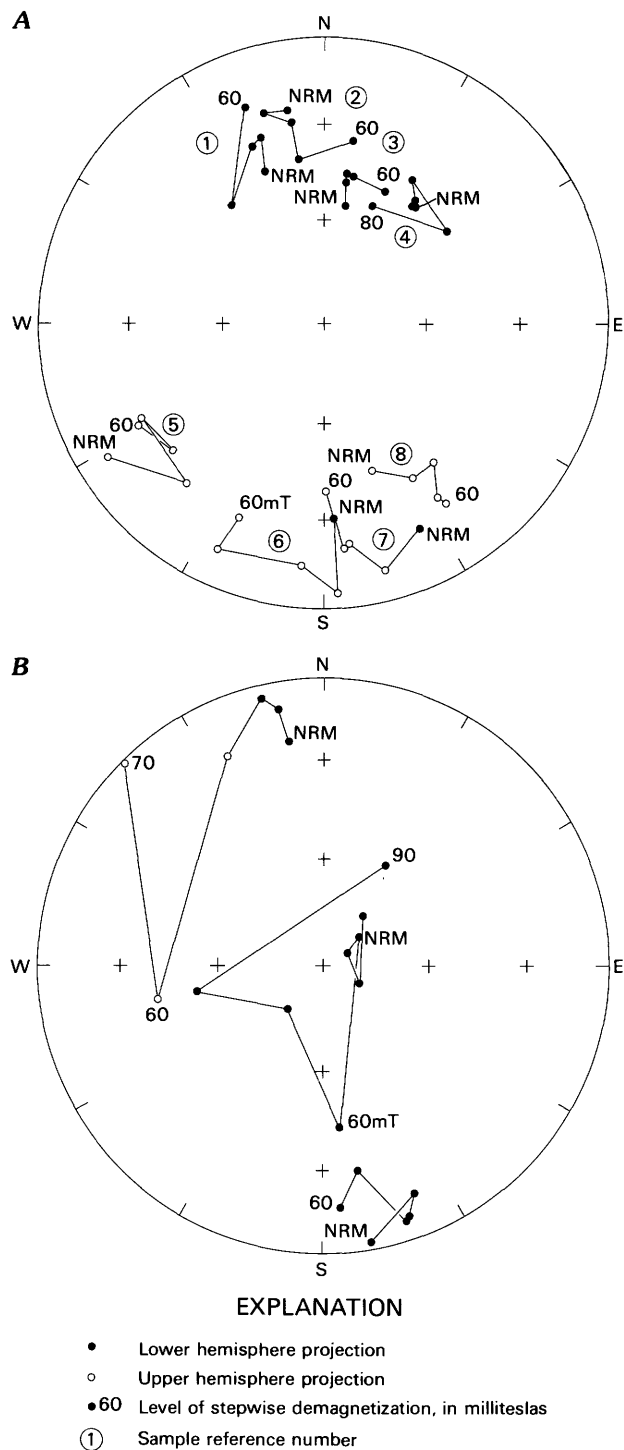
Figure 11. Equal-area projections of magnetic remanence in samples showing normal (N), reversed (R), and indeterminate (I) polarities. A, samples yielding single component N polarity (1-4) and R polarity (5-8); B, samples yielding I polarity. Sample remanence was measured prior to demagnetization (NRM) and at a minimum of four levels of AF demagnetization: 10, 20, 40, and 60 mT (milliteslas).

In reversed samples, magnetic intensity commonly increased after each of the first few steps of AF or thermal demagnetization. Fifty-eight percent of the R samples showed an increase in magnetic intensity during demagnetization. Intensity peaks during demagnetization suggest that antiparallel magnetic vectors were removed at low levels of demagnetization. These intensity increases commonly coincided with a change from normal or intermediate vector directions to consistent reversed directions (fig. 13). In contrast, only 7 percent of the N samples showed post-NRM intensity peaks. Notably, these normal samples were located in the upper 5 m of the Gauss Polarity Chronozone and in a normal horizon in the Matuyama Polarity Chronozone, where the sediments were presumably most susceptible to magnetic overprinting. In summary, reversed magnetic components were generally not apparent in normal samples, whereas normal magnetic components were commonly removed during demagnetization of reversed samples.

The decrease in magnetic intensity upon thermal demagnetization of the drill core samples provides some indication of the source of magnetic remanence in the basin-fill sediments. Thermal demagnetization to 200 °C removed about 35–60 percent of the NRM in most of the samples (fig. 14), suggesting the presence of goethite (Neel temperature, 120 °C). About 5–20 percent of the NRM was removed between 500° and 600 °C, suggesting some contribution from magnetite (Curie temperature, 580 °C), although remnents of unaltered magnetite were sparse in polished sections of the sediments. After demagnetization to 600 °C, about 20–60 percent of the NRM remained in the samples, which suggests that hematite (Neel temperature, 680 °C) contributes to the magnetic remanence of the samples. Magnetic intensity changes resulting from thermal demagnetization of the eight core samples suggest that hematite, goethite, and perhaps magnetite contribute to the magnetic remanence in the basin-fill deposits.

The mean inclination of sample remanence in N and R samples, based on measurements after demagnetization at 20 mT (or 200 °C) and 60 mT (or 600 °C), was about 17° shallower than the inclination of the axial dipole field (58°) at the sampling site. The range of differences between measured inclinations and the inclination predicted by the axial dipole model is similar in magnitude to an "inclination error," commonly associated with depositional remanent magnetization (DRM) in silts and sands (King, 1955; Griffiths and others, 1957; Rees, 1961). The differences in inclination between N and R samples (table 3) may in part reflect depositional effects, but they may also be related to normal-polarity overprints in the reversed samples.
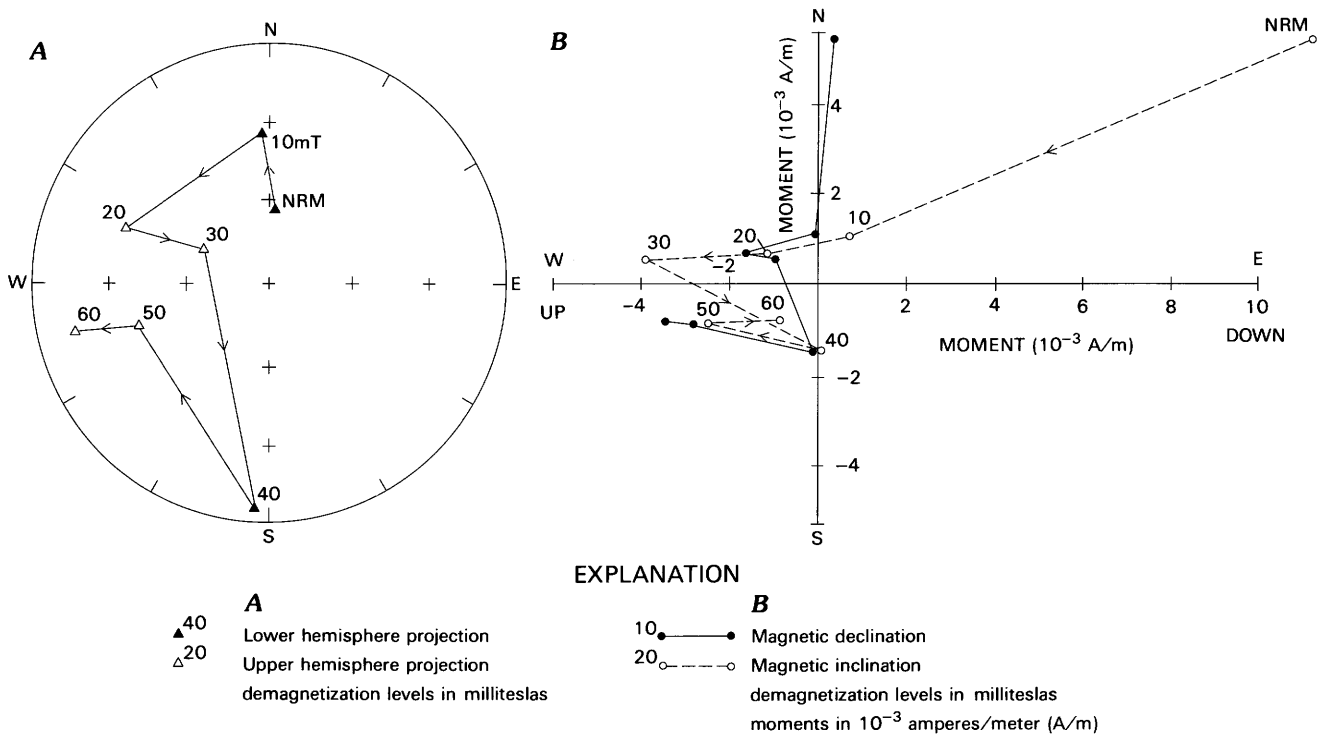
Figure 12. Projections of magnetic remanence from a sample containing multiple-polarity components. *A,* equal area projection; *B,* orthogonal projection. The projections indicate a reversed-polarity component (40 to 60 mT) in addition to a normal-polarity overprint (NRM to 30 mT) that was removed upon stepwise AF demagnetization.
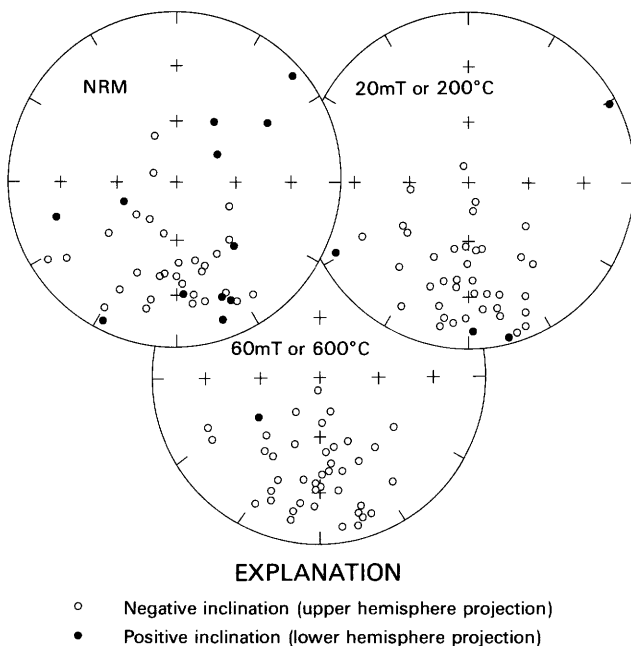
Figure 13. Equal-area projection of magnetic remanence in reversed samples at natural remanent magnetism and during stepwise demagnetization.

Petrography

Polished thin sections from indurated hand specimens were examined under reflected light to identify magnetic minerals in the basin-fill sediments. Detrital grains of specular hematite are abundant in the polished sections. The detrital hematite, about 3–100 μm in diameter, consists predominantly of martite (pseudomorphic hematite after magnetite) with little or no relict magnetite. Most of the detrital hematite grains are much smaller than the adjacent silicate grains. Hematite also occurs as thin coatings on specular hematite, biotite, and other iron-bearing minerals.

Dominant grain size was determined for 103 (61 percent) of the paleomagnetic samples, including at least one sample from each of the horizons shown in figure 9. The dominant grain size in the samples ranges from very fine to medium sand (fig. 15A). Both the reliability of polarity interpretations and the geometric mean NRM intensities of samples in the grain-size classes decrease with increasing grain size (figs. 15B and C). Differences between the mean NRM intensities of samples in the grain-size classes were evaluated using analysis of variance (ANOVA) and the Student–Newman–Keuls multiple

Table 2. Variation in magnetic intensity related to polarity of the Fisher Valley sediments

[NRM intensity was measured prior to demagnetization and the maximum intensity was the maximum observed during stepwise demagnetization. NRM, natural remanent magnetization; A/m, amperes/meter]

Polarity classification	Geometric mean of NRM intensities (10^{-3} A/m)	Geometric mean of maximum intensities (10^{-3} A/m)	Number of samples
By Polarity Chronozone:			
Brunhes	3.0	3.0	23
Matuyama	1.8	2.0	125
Gauss	4.5	4.7	20
			168
By sample:			
Normal	3.7	3.7	44
Normal(?)	2.1	2.2	14
Reversed	1.9	2.2	44
Reversed(?)	1.6	1.9	21
Indeterminate	1.7	1.9	45
			168

Table 3. Inclination of remanence related to polarity
[Comparison was restricted to samples showing only one polarity component during stepwise demagnetization. mT, milliteslas; $\bar{x}$, mean; s, standard deviation; n, number of samples]

Sample polarity	Measured inclinations minus axial dipole inclination (58°) in degrees					
	20 mT or 200 °C			60 mT or 600 °C		
	$\bar{x}$	s	n	$\bar{x}$	s	n
Normal (N)[1]	8.5	14.3	35	13.3	18.7	32
Reversed (R)	23.0	21.4	44	21.7	19.1	43

[1]Normal samples in Matuyama Polarity Chronozone were omitted due to possible overprints.

comparison of sample means (Zarr, 1974). Assuming the grain-size samples are random, the mean NRM intensity of the very fine grained samples is significantly higher ($\alpha = 0.001$) than that of the fine- and the medium-grained samples. The mean NRM intensities of fine- and medium-grained samples were not significantly different ($\alpha = 0.05$).

Interpretation of Remanence

The magnetic mineralogy and magnetic characteristics of the paleomagnetic samples strongly suggest that the primary magnetization in the basin-fill sediments is a DRM carried by detrital specular hematite. The basis for this interpretation is as follows. Highly altered detrital specular hematite is abundant in polished sections of the sediments. The magnetic minerals in the deposits are similar to those described for the source rocks which in-

dicates that these minerals have not undergone significant post-depositional alteration. The detrital hematite grains are of a size range that could have become oriented within the interstices of the larger sand-sized particles at the time of deposition. Intensity changes upon demagnetization also indicate that part of the remanence is carried by hematite. Most of the reversed and normal polarities in the deposits remained stable throughout demagnetization and subsequently defined distinct polarity zones in the stratigraphic section. Furthermore, the magnetic inclination in samples containing single-polarity components (N and R samples) is shallower than the inclination of the axial dipole field. The shallow inclinations are suggestive of inclination error that often results from DRM. Lastly, the Brunhes-Matuyama polarity boundary (0.73 m.y.) in the sediments is located near the 0.73 m.y.-old Bishop ash, which indicates that the sediments were magnetized near the time of deposition.
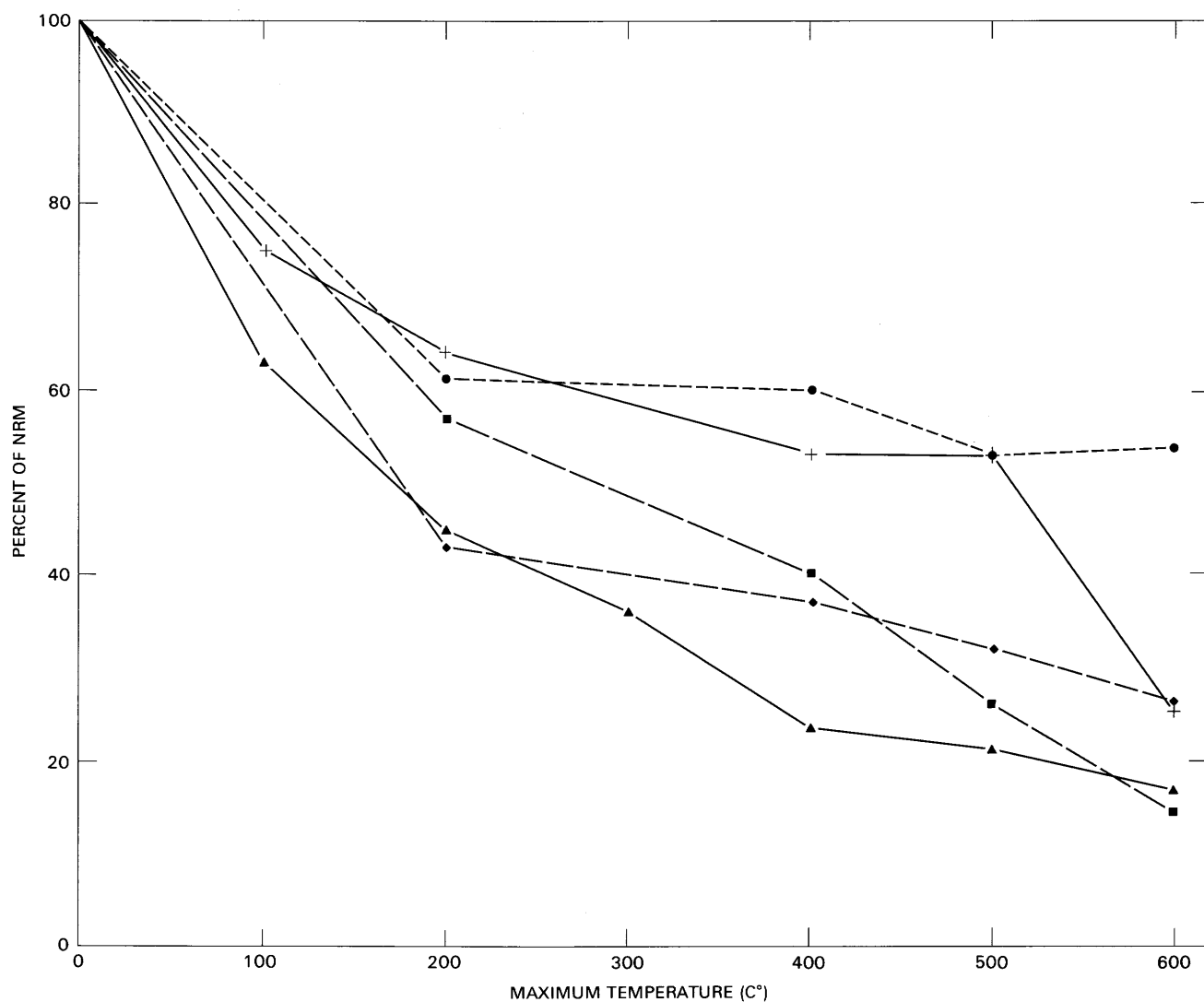
Figure 14. Magnetic intensity changes in five cores from unit QTbl subjected to stepwise thermal demagnetization.

However, magnetic overprints in some of the paleomagnetic samples suggest that a secondary chemical remanent magnetization (CRM) and (or) viscous remanent magnetization (VRM) has altered the primary depositional remanence. Multiple-polarity components in sediments in the reversed-polarity zone indicate a post-depositional secondary magnetization. These samples showed directional changes, from normal to reversed, coincident with an increase in magnetic intensity upon demagnetization. Several sampled horizons in the reversed-polarity chronozone contain both normal and reversed polarities, suggesting normal-polarity remagnetization. The anomalously shallow inclination of R samples compared to that of N samples (table 3) is consistent with models of chemical overprinting (Patterson, 1981; Larson and Walker, 1982), in which dominantly reversed directions are effectively "pulled" towards shallower directions by normal polarity components.

Hematite replacements of biotite or remanents of magnetite in detrital hematite and hematite films around grains of specular hematite or biotite could carry a post-depositional CRM if this hematite formed after deposition. It is difficult to determine which iron-oxide minerals formed in situ because similar hematite minerals occur in the source rocks. However, on the basis of the high degree of weathering of magnetic minerals in the source beds and the abundance of detrital hematite grains in the Fisher Valley sediments, the primary remanence appears to be related to the detrital hematite.

Magnetostratigraphy

Sample polarities and the interpreted magnetic stratigraphy of the composite stratigraphic section are shown in figure 9. Seventy-three percent of the samples
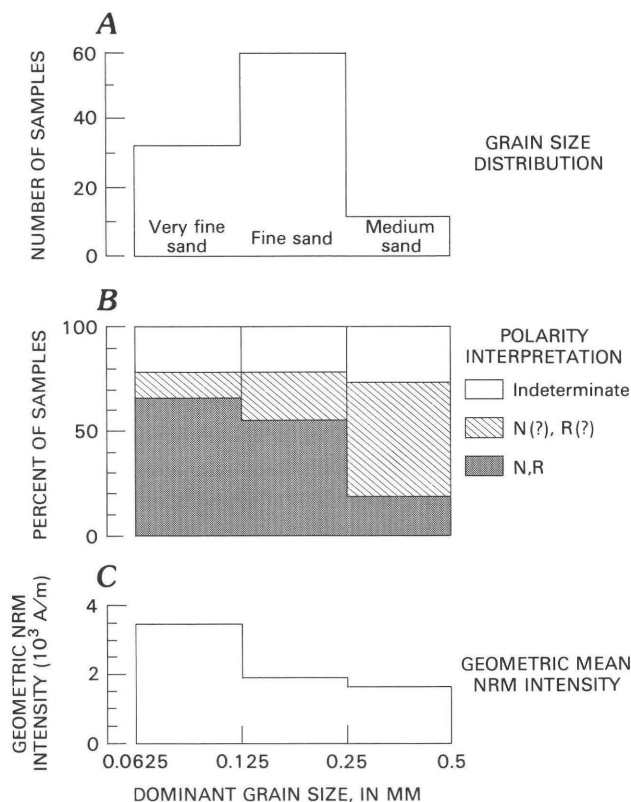
Figure 15. *A*, grain-size distribution of paleomagnetic samples related to *B*, interpreted polarity and *C*, intensity of natural remanent magnetism.

yielded interpretable (N, N?, R, R?) polarities. The composite section contains three major polarity zones forming a normal-reversed-normal sequence. These appear to represent the Brunhes (normal), Matuyama (reversed), and Gauss (normal) Polarity Chronozones based on the magnetic stratigraphy and other evidence presented in the following discussion. The Brunhes-Matuyama boundary occurs in section A about 27 m below the Lava Creek ash and in section B about 5 m below the Bishop ash and 30 m below the Lava Creek ash. Minimum thicknesses of the Brunhes, Matuyama, and Gauss Polarity Chronozones are 76, 45, and 20 m, respectively. The actual thicknesses of the Matuyama and Gauss units are difficult to estimate because (1) the exact correlation between sections A and B, which contain the top of the Matuyama, and section C, which contains the base of the Matuyama, is uncertain; and (2) the base of the sediments deposited during the Gauss Polarity Chronozone is not exposed.

The age of the Brunhes-Matuyama boundary has been estimated to be 0.73 m.y. (Mankinen and Dalrymple, 1979). Our interpretation of the Brunhes-Matuyama polarity boundary in the Fisher Valley sediments is based largely on the proximity of the polarity change to the radiometrically dated Lava Creek and Bishop ashes (0.61 and 0.73 m.y., respectively; Izett,

1981). Although the Bishop ash was not found in section A, the distances between the N/R polarity boundary and the Lava Creek ash are similar in sections A and B (fig. 9).

Geologic mapping (Colman and Hawkins, 1985) indicates that most of section C underlies sections A and B. The older age for section C, the relative thicknesses of the reversed and lower normal polarity units, and the uniform polarities within the lower normal polarity unit suggest that the lowermost sediments in section C were deposited during the Gauss Polarity Chronozone. This interpretation also allows for the possibility that one or more of the normal horizons within the Matuyama Polarity Chronozone represent normal-polarity subchronozones.

Normal polarities were generally well resolved and consistent throughout the Brunhes and Gauss polarity units. The resolution of polarities was less consistent in the Matuyama Polarity Chronozone. Reliable polarities (N, R) represent more than 70 percent of the samples in the normal (Brunhes and Gauss) polarity zones compared to 40 percent in the reversed (Matuyama) polarity zone, and the reversed-polarity zone contains a higher proportion of samples showing indeterminate polarities. Seven subzones within the reversed-polarity zone contain normally magnetized samples, and several horizons contain both normal and reversed samples (fig. 9). The normal polarities and the polarity conflicts might be the result of younger normal remagnetization of portions of these subzones. Evidence that suggests partial remagnetization of reversed samples is presented in the Discussion section. Some of the normal polarities in the Matuyama Polarity Chronozone may reflect deposition during normal-polarity subchronozones; however, this conclusion is tenuous because of the lack of detailed independent age control and because of the possibility of younger normal remagnetization.

Discussion

The timing and processes by which red sediments acquire remanent magnetization are subjects of considerable debate (Collinson, 1965; Turner, 1979; Van Houten, 1968; and others). Several studies addressing this problem have been conducted on one of the source rocks for the Fisher Valley sediments, the Triassic Moenkopi Formation, in which the magnetization has been attributed to both DRM (Elston and Purucker, 1979) and CRM (Larson and others, 1982). Studies of first-cycle red beds of late Cenozoic age indicate that chemical remagnetization can occur as much as 20 m.y. after deposition (Hoblitt and others, 1974), can take place at a nonuniform rate, and can effectively obscure primary depositional remanence (Larson and Walker, 1975). The magnetic stratigraphy in the Fisher Valley sediments

offers some insight into the acquisition and long-term stability of magnetic remanence in second-generation red-bed deposits.

The coarse-grained, fluvial sediments in Fisher Valley apparently became magnetized near the time of deposition and, if our interpretation of the magnetic stratigraphy is correct, have carried a stable remanence for more than 2.5 m.y. The DRM in such sediments can result from the alignment of fine-grained magnetic particles within the interstices of the sand-sized particles, during or soon after deposition. In contrast to first-cycle red sediments, the preservation of primary remanence in these second-cycle red beds appears to be due partly to the highly oxidized state of magnetic minerals prior to deposition and partly to the pervasive calcium carbonate cement in the deposits. Rates of authigenesis and chemical remanence acquisition should decrease with decreasing amounts of unaltered iron-bearing minerals. In addition, calcium carbonate cement can protect partially altered minerals from further alteration by limiting ground-water infiltration (Walker and others, 1978).

However, some of the sediments in the Matuyama polarity unit do show evidence of partial remagnetization. N and R samples in single sampled horizons from this zone suggest that the overprints can effectively cancel the primary detrital remanence. The overprints could result from either viscous or chemical remagnetization of the sediments. In the Fisher Valley sediments we cannot distinguish between VRM or CRM, and both may be present. Hematitic sediments can acquire a VRM (Dunlop and Sterling, 1977) but the process is not well understood. Chemical components may have resulted from in-situ alteration of incompletely oxidized detrital ferrous iron-bearing minerals or from interstitial ferric oxyhydroxide phases formed locally from redistributed iron (Larson and others, 1982; Walker and others, 1981). Unaltered magnetite within detrital grains of hematite (martite) and grains of biotite are two possible sources in the Fisher Valley sediments for remanence acquisition. Mineralogic sources of magnetic remanence in red sediments are difficult to identify positively (Walker and others, 1981; Collinson, 1983). It is especially difficult to recognize minerals carrying magnetic components in second-cycle red beds because the sediments are derived from deposits which contain authigenic iron oxides.

Indeterminate sample polarities could also be caused by mechanical reorientation of magnetic particles during deposition or by the presence of highly magnetized sandstone clasts in the samples. Sandstone fragments, generally less than 3 mm in diameter, occur locally in the deposits. Although we avoided sampling material that contained large bedrock fragments, small strongly magnetized fragments could significantly affect sample remanence (Larson and others, 1982; Larson, 1981).

Although some of the sediments in the Gauss Polarity Chronozone showed an increase in magnetic intensity upon demagnetization, none of the samples showed clear directional evidence of multiple polarity components. Probably all polarity zones have acquired a CRM and (or) a VRM, but only the Matuyama Polarity Chronozone contains clear evidence of multiple polarity components. The absence of reversed magnetic components in the older Gauss polarity unit may result from (1) the cancellation of reversed overprints by younger normal overprints acquired during the Brunhes Polarity Chronozone or (2) the change in hydrological conditions in the deposits that occurred during the Brunhes that perhaps accelerated rates of authigenesis.

If the sediments can acquire a CRM or VRM over short time intervals, on the order of less than a few hundreds of thousands of years, the normal sediments in the Gauss unit may have once carried a reversed CRM acquired during the Matuyama Polarity Chronozone. During the Brunhes Polarity Chronozone, a second overprint, this time normal, may have effectively cancelled the former reversed overprint. The sediments in the Gauss Polarity Chronozone presently carry a single-component, normal remanence.

Alternately, the remagnetization in the Matuyama Polarity Chronozone, and the lack of such overprint in the older Gauss Polarity Chronozone may be related to drainage incision of Onion Creek. Radiocarbon dates on organic material in sediments related to the incision suggest that much of the incision occurred during the past 10,000 years. (See Physical Stratigraphy section.) Chemical remagnetization in the Matuyama unit may be due to changes in chemical conditions in the deposits resulting from lowering of the ground-water table with the drainage incision. If a change in ground-water level and chemistry accelerated authigenesis, recent normal chemical remagnetization would be most advanced in the uppermost reversed sediments. Both normal and indeterminate sample polarities are more common in the upper part of the Matuyama Polarity Chronozone than in the lower portion of this zone (fig. 9). Local variations in cementation or magnetic mineralogy of the sediments, which can affect rates of authigenesis, could also be related to the acquisition of a CRM.

Summary

The sediments in Fisher Valley yield a magnetic polarity stratigraphy which we interpret as the Brunhes, Matuyama, and Gauss Polarity Chronozones. Minimum thicknesses of the sediments deposited during the polarity chronozones are 76, 45, and 20 m, respectively. The Brunhes-Matuyama boundary is located about 5 m below the Bishop ash and about 30 m below the Lava Creek

ash. Normal polarities within the Matuyama Polarity Chronozone may represent normal-polarity subchronozones, but the lack of detailed independent age control and evidence of post-depositional remagnetization in the reversed zone prevent positive identification of such events. Polarity subzones may be delineated in such deposits where independent age control exists.

The magnetic remanence in the sediments is apparently a depositional, detrital remanent magnetization carried primarily by specular hematite. Stability of the magnetic remanence appears to be related both to the grain size of the deposits and to local remagnetization. VRM and (or) CRM can apparently be acquired by such sediments over periods of about 1 m.y. or less. If our interpretation of the magnetic stratigraphy is correct, the sediments in the lower exposed basin-fill deposits have carried a DRM for at least 2.5 m.y. We attribute the preservation of the DRM in the second-cycle red sediments to the highly altered condition of the magnetic minerals prior to deposition and to the pervasive calcium carbonate cement in the deposits. The magnetic stratigraphy of the upper Cenozoic deposits in Fisher Valley provides an age framework for sediments that otherwise contain few datable materials.

In conclusion, the stable magnetization in the Fisher Valley sediments demonstrates the usefulness of magnetic stratigraphy for dating young, second-cycle red beds. However, evidence of post-depositional remagnetization of the sediments in the reversed-polarity zone (Matuyama Polarity Chronozone) suggests that the preservation of a DRM can be variable in such deposits.

LATE CENOZOIC DEPOSITIONAL HISTORY OF THE FISHER VALLEY AREA

The upper Cenozoic sediments in Fisher Valley result from a long history of deposition, deformation, and geomorphic changes related to movement of the Onion Creek diapir (Colman, 1983). The physical, soil, and paleomagnetic stratigraphy of the Fisher Valley sediments form the primary record of this history.

Mesozoic rocks arched over the crest of the Fisher Valley anticline probably began to collapse in late Miocene or early Pliocene time because of solution and flowage of the salt core in response to late Miocene uplift of the Colorado Plateau (Cater, 1970; Hunt, 1956). Beheaded remnants of consequent stream channels flowing away from the crest of the anticline are preserved in the Mesozoic rocks that form dip slopes on the northeast and southwest flanks of the anticline (Colman, 1983). Ancestral Fisher Creek headed in the igneous rocks of the La Sal Mountains, flowed through the collapsed crest of the anticline in Fisher Valley, and followed the present course of Onion Creek to the Colorado River (fig. 1).

The Pliocene(?) gravels that contain igneous clasts from the La Sal Mountains must have been deposited by Fisher Creek against the exposed cap rock of the Onion Creek diapir; these gravels are the primary evidence for the former course of Fisher Creek (Colman, 1983). Prior to late Pliocene time, Beaver Creek apparently captured the headwaters of ancestral Fisher Creek, as late Pliocene basin-fill sediments deposited by Fisher Creek do not contain igneous clasts from the La Sals.

In late Tertiary time, the Onion Creek salt diapir began to move upward, probably in response to unloading of overburden after anticlinal collapse, although other causative mechanisms may have been involved (Colman, 1983). The upward movement of the diapir created a depositional basin to the east and impeded the flow of Fisher Creek, causing deposition and progressive deformation of a thick sequence of basin-fill sediments. Magnetic stratigraphy suggests that the lower basin-fill deposits belong to the Gauss Polarity Chronozone; if so, movement of the diapir began before about 2.5 m.y. ago. Deposition of the basin-fill sediments was controlled by pulses of diapiric movement and by climatic change, resulting in upward-fining sedimentary units interrupted by buried soils that indicate periods of landscape stability.

The pattern of deformation of the deposits clearly shows upward movement of the diapir in an absolute sense (Colman, 1983) and suggests that the movement was punctuated by sporadic surges. The Pliocene(?) gravels at the base of the sedimentary sequence are sharply infolded into the cap rock with complex, near-vertical contacts (fig. 4). The lower unit of the basin-fill sediments dips radially away from the diapir and locally dips toward the valley walls in excess of 20°. The upper unit of the basin-fill sediments are tilted as much as 10°, also locally toward the valley walls. At least four angular unconformities along the margins of the sedimentary basin, coupled with concordant deposition towards the basin center, suggest episodic subsidence of the depositional basin. The overall pattern of deformation suggests minimum upward movement of the diapir and minimum subsidence of the sedimentary basin of about 70 m each, representing at least 140 m of total differential movement (Colman, 1983).

The angular unconformities along the basin margins mark pulses of deformation. One major angular unconformity separates the upper and lower units of the basin-fill deposits and is thus bracketed by the Lava Creek and Bishop ashes (0.61 and 0.73 m.y., respectively; Izett, 1981). The well-developed buried soil (soil C) at the top of the lower basin-fill unit suggests that the angular unconformity is close to the Lava Creek ash in age. Other angular unconformities, which occur in both the upper and the lower basin-fill units, are at stratigraphic positions that are difficult to trace to the ashes and buried soils preserved near the center of the basin. Their ages

are thus uncertain, except for the limits provided by the ages of the depositional units.

Ages estimated from the secondary carbonate content of the soil (soil I) that caps the basin-fill sediments suggest that deposition ended about 0.26 m.y. ago. Uranium-trend analyses suggest an age of about 0.24 m.y. ago for this event. The end of basin-fill deposition was probably caused by filling of the depositional basin to the point where Fisher Creek was diverted northeastward into the structural and topographic low of Cottonwood graben and thence to the Dolores River. Since that time, Onion Creek, eroding headward from the Colorado River along the course of ancestral Fisher Creek, has cut across the Onion Creek diapir and into the basin-fill sediments. At present, Onion Creek is within 1.5 km of capturing Fisher Creek and restoring it to its ancestral course. The only deposits in Fisher Valley younger than the basin-fill sediments are minor amounts of inset fluvial deposits (unit Qas) and Holocene alluvium and eolian sand.

The upper Cenozoic deposits in Fisher Valley have recorded the history of the valley and its relation to the Onion Creek salt diapir. Geologic mapping and analysis of the physical and soil stratigraphy provided the sequence of events in the history of Fisher Valley and the relation of the landforms and deposits to movement of the diapir. Analyses of soil development and paleomagnetic stratigraphy provided most of the time framework into which the sequence of events fits.

REFERENCES CITED

Biggar, N. E., Harden D. R., and Gillam, M. L., 1981, Quaternary deposits in the Paradox Basin, *in* Weigand, D. L., ed., Geology of the Paradox Basin: Rocky Mountain Association of Geologists, 1981 Field Conference, p. 129-145.

Birkeland, P. W., 1984, Soils and geomorphology: New York, Oxford University Press, 372 p.

Carter, W. D., and Gualtieri, J. L., 1965, Geyser Creek fanglomerate (Tertiary), La Sal Mountains, eastern Utah: U.S. Geological Survey Bulletin 1224-E, p. E1-11.

Cater, F. W., 1970, Geology of the salt anticline region in southwestern Colorado: U.S. Geological Survey Professional Paper 637, 80 p.

Channel, J. E. T., 1982, Paleomagnetic stratigraphy as a correlation technique, *in* Odin, G. S., ed., Numerical dating in stratigraphy: New York, John Wiley and Sons, Ltd., p. 81-103.

Chleborad, A. F., Powers, P. S., and Farrow, R. A., 1975, A technique for measuring bulk volume of rock materials: Association of Engineering Geologists Bulletin, v. 12, no. 4, p. 317-322.

Choquette, A. F., and Colman, S. M., 1983, Paleomagnetic stratigraphy of Upper Cenozoic sediments, Fisher Valley, southeastern Utah: Geological Society of America Abstracts with Programs, v. 15, p. 388.

Collinson, D. W., 1965, The remanent magnetization and magnetic properties of red sediments: Geophysical Journal, Royal Astronomical Society, v. 10, p. 105-126.

———1983, Methods in rock magnetism and paleomagnetism—Techniques and instrumentation: London, Chapman and Hall, 503 p.

Colman, S. M., 1983, Influence of the Onion Creek salt diapir on the late Cenozoic history of Fisher Valley, southeastern Utah: Geology, v. 11, p. 240-243.

Colman, S. M., and Hawkins, F. F., 1985, Surficial geologic map of the Fisher Valley-Professor Valley area, southeastern Utah: U.S. Geological Survey Miscellaneous Investigations Map I-1596, scale: 1-24,000.

Dane, C. H., 1935, Geology of the salt anticline and adjacent areas, Grand County, Utah: U.S. Geological Survey Bulletin 863, 184 p.

Dreimanis, Aleksis, 1962, Quantitative determination of calcite and dolomite by using Chittick apparatus: Journal of Sedimentary Petrology, v. 32, no. 8, p. 520-529.

Dunlop, D. J., and Sterling, J. M., 1977, 'Hard' viscous remanent magnetization (VRM) in fine-grained hematite: Geophysical Research Letters, v. 4, no. 4, p. 163-166.

Elston, D. P., and Purucker, M. F., 1979, Detrital magnetization in red beds of the Moenkopi Formation (Triassic), Gray Mountain, Arizona: Journal of Geophysical Research, v. 84, no. B4, p. 1653-1665.

Gile, L. H., and Grossman, R. B., 1979, The Desert Project soil monograph: U.S. Department of Agriculture, Soil Conservation Service, 984 p.

Gile, L. H., Hawley, J. W., and Grossman, R. B., 1981, Soils and geomorphology in the Basin and Range area of southern New Mexico—Guidebook to the Desert Project: New Mexico Bureau of Mines and Mineral Resources Memoir 39, 222 p.

Griffiths, D. H., King, R. F., and Wright, A. E., 1957, Some field and laboratory studies of depositional remanence of recent sediments: Advances in Physics, v. 6, p. 306.

Griffiths, D. H., King, R. F., Rees, A. I., and Wright, A. E., 1960, Remanent magnetism of some recent varved sediments: Proceedings of the Royal Society of London, Series A, v. 256, p. 359-383.

Guthrie, R. L., and Witty, J. E., 1982, New designations for soil horizons and layers and the new Soil Survey Manual: Soil Science Society of America Journal, v. 46, p. 443-444.

Harden, D. R., Biggar, N. E., and Gillam, M. L., 1985, Quaternary deposits and soils in and around Spanish Valley, Utah, *in* Weide, D. L., ed., Soils and Quaternary geology of the southwestern United States: Geological Society of America Special Paper 203, p. 43-64.

Hays, J. D., Imbrie, John, and Shackleton, N. J., 1976, Variations in the earth's orbit—Pacemaker of the ice ages: Science, v. 194, no. 4270, p. 1121-1132.

Hoblitt, R. P., Larson, E. E., and Walker, T. R., 1974, Chemical remagnetization of Miocene red beds in southern New Mexico [abs.]: Eos, Transactions of the American Geophysical Union, v. 55, no. 12, p. 1110.

Hunt, C. B., 1956, Cenozoic geology of the Colorado Plateau: U.S. Geological Survey Professional Paper 279, 99 p.

Izett, G. A., 1981, Volcanic ash beds—Recorders of upper Cenozoic silicic pyroclastic volcanism in the western United States: Journal of Geophysical Research, v. 86, no. B11, p. 10200-10222.

King, R. F., 1955, The remanent magnetism of artificially deposited sediments: Royal Astronomical Society, Monthly Notices, Geophysical Supplement, v. 7, no. 3, p. 115-134.

Larson, E. E., 1981, Selective destructive demagnetization—Another microanalytic technique in rock magnetism: Geology, v. 9, p. 350-355.

Larson, E. E., and Walker, T. R., 1975, Development of chemical remanent magnetization during early stages of red-bed formation in late Cenozoic sediments, Baja, California: Geological Society of America Bulletin, v. 86, p. 639-650.

———1982, A rock magnetic study of the lower massive sandstone, Moenkopi Formation (Triassic), Gray Mountain area, Arizona: Journal of Geophysical Research, v. 87, no. B6, p. 4819-4836.

Larson, E. E., Walker, T. R., Patterson, P. E., Hoblitt, R. P., and Rosenbaum, J. G., 1982, Paleomagnetism of the Moenkopi Formation, Colorado Plateau—Basis for longterm model of acquisition of chemical remanent magnetism in red beds: Journal of Geophysical Research, v. 87, no. B2, p. 1081-1106.

Levine, E. R., and Ciolkosz, E. J., 1983, Soil development on till of various ages in northeastern Pennsylvania: Quaternary Research, v. 19, no. 1, p. 85-99.

Machette, M. N., 1978, Dating Quaternary faults in the southwestern United States by using buried calcic paleosols: U.S. Geological Survey Journal of Research, v. 6, no. 3, p. 369-381.

Machette, M. N., 1985, Calcic soils of the American Southwest, in Weide, D. L., ed., Soils and Quaternary geology of the southwestern United States: Geological Society of America Special Paper 203, p. 1-21.

Mankinen, E. A., and Dalrymple, G. B., 1979, Revised geomagnetic polarity time scale for the interval 0-5 m.y. B. P.: Journal of Geophysical Research, v. 84, no. B2, p. 615-626.

National Oceanic and Atmospheric Administration, 1981, Climatic data for the United States, annual summaries: v. 13, 563 p.

Patterson, P. E., 1981, Petrographic, geochemical, and paleomagnetic study of color banding the Cathedral Bluffs Tongue of the Wasatch Formation (Eocene), Washakie Basin, Wyoming: Boulder, Colo., University of Colorado, M.S. thesis, 151 p.

Pierce, K. L., 1979, History and dynamics of glaciation in the northern Yellowstone National Park area: U.S. Geological Survey Professional Paper 729-F, 90 p.

Rees, A. I., 1961, The effect of water currents on the magnetic remanence and anisotropy of susceptibility of some sediments: Geophysical Journal, Royal Astronomical Society, v. 5, p. 235-251.

Richmond, G. M., 1962, Quaternary stratigraphy of the La Sal Mountains, Utah: U.S. Geological Survey Professional Paper 324, 135 p.

Rosholt, J. R., 1985, Uranium-trends systematics for dating Quaternary sediments: U.S. Geological Survey Open-File Report 85-298, 34 p.

Shoemaker, E. M., 1954, Structural features of southeastern Utah and adjacent parts of Colorado, New Mexico, and Arizona, in Stokes, W. L., ed., Guidebook to the geology of Utah: Utah Geological Society, Guidebook 9, p. 48-69.

Turner, P., 1979, The paleomagnetic evolution of continental red beds: Geological Magazine, v. 116, no. 4, p. 289-301.

U.S. Department of Commerce, Weather Bureau, 1953, Climatic summary for the United States, supplement for 1931-1952, 337 p.

Van Houten, F. B., 1968, Iron oxides in red beds: Geological Society of America Bulletin, v. 79, p. 399-416.

Verosub, K. L., 1977, Depositional and post-depositional processes in the magnetization of sediments: Reviews of Geophysics and Space Physics, v. 15, p. 129-143.

Walker, T. R., Larson, E. E., and Hoblitt, R. P., 1981, Nature and origin of hematite in the Moenkopi Formation (Triassic), Colorado Plateau—A contribution to the origin of magnetism in red beds: Journal of Geophysical Research, v. 86, no. B1, p. 317-333.

Walker, T. R., Waugh, Brian, and Crone, A. J., 1978, Diagenesis in first-cycle desert alluvium of Cenozoic age, southwestern United States and northwestern Mexico: Geological Society of America Bulletin, v. 89, p. 19-32.

Zarr, H. E., 1974, Biostatistical analysis: Englewood Cliffs, New Jersey, Prentice-Hall Inc., 620 p.

Zijderveld, J. D. A., 1967, A. C. demagnetization of rocks—Analysis of results, in Collinson, D. W., Creer, R. M., and Runcorn, S. K., eds., Developments in solid earth geophysics, v. 3, Methods in paleomagnetism: Amsterdam, Elsevier, p. 254-286.

TABLES 4–6

Descriptions and laboratory data, Fisher Valley soils

Table 4. Soil descriptions and laboratory data, Fisher Valley soils

[All soils located in section A (fig. 3), except for soil I gravelly facies, which is located near the basin margin; n.d., not determined]

Sample	horizon[1]	Depth (cm)	Texture[2]	Color[3] (dry)	Structure[4]	Carbonate morphology[5]	Weight percent gravel	Sand Coarse	Sand Fine	Silt Coarse	Silt Fine	Clay Coarse	Clay Fine	Total clay (g/cm³)	Bulk density[7] (g/cm³)	Percent CaCO₃ (<2mm)	Weight loss on ignition
											Weight percent[6]						
								Soil J									
SJ-1	A1	0-8	sl	5YR5/5	sg-w,vf,pl	none	0.0	3.1	59.3	19.6	7.5	6.0	4.5	0.15	1.4[e]	6.7	2.8
SJ-2	A1	8-18	l	5YR5/4	w,vf,pl	none	.0	2.0	46.6	26.3	11.9	8.6	4.7	.19	1.43	6.4	3.0
SJ-3	Ck1	18-42	sl	2.5YR5/5	m,c,abk	none	.0	3.9	65.7	20.2	3.9	3.7	2.6	.09	1.47	8.4	1.4
SJ-4	Ck2	42-72	sl	2.5YR5/5	w,m-c,abk	none	.0	3.6	67.5	19.5	3.8	3.3	2.3	.08	1.43	7.6	1.2
								Soil I									
SI-1	Btb	0-20	sl	5YR5/5	s,m,abk	I	0.0	2.5	58.1	19.3	4.1	3.4	12.6	0.28	1.76	0.6	1.4
SI-2	BKb1	20-43	sl	5YR5/6	s,f,abk	I	.0	1.3	53.4	20.9	5.3	17.0	2.1	.35	1.81	1.2	1.9
SI-3	Btkb2	43-67	l	5YR5/6	s,m,abk	I	.0	1.0	42.5	28.6	6.5	5.9	15.4	.39	1.82	2.3	2.3
SI-4	BKb	67-93	l	5YR5/7	m,m,sbk	I	.0	.9	45.8	28.3	8.8	9.8	6.4	.28	1.68	3.1	2.0
SI-5	KBb	93-109	sl	5YR6/5	m,m,pl	III-	.0	10.2	55.6	13.0	3.2	4.2	13.9	.32	1.72	39.4	2.1
SI-6	Kb1	109-135	sl	5YR8/5	m,c,pl	III	.0	10.6	53.5	18.2	3.3	5.0	9.4	.25	1.69	37.0	.9
SI-7	Kb2	135-170	sl	5YR7/4	s,m,pl	III	.0	11.9	57.7	15.7	2.8	2.6	9.4	.23	1.91	24.5	.7
SI-8	Ckb1	170-218	sl	5YR5/6 / 5YR7/4[a]	s,c,pl- / m,m,abk	II-III	.0	12.4	54.9	21.5	4.0	3.5	3.6	.14	1.89	18.2	.8
SI-9	Ckb2	218-248	sl	5YR5/5 / 5YR6/4[a]	s,m,abk	II	.0	10.6	49.7	28.7	4.8	3.2	3.0	.11	1.81	12.0	.7
SI-10	Ckb3	248-282	sl	2.5YR5/6	m-s,m,abk	I	.0	12.7	49.4	26.1	4.8	3.5	3.6	.13	1.81	14.4	.6
SI-11	Ckb4	282-317	sl	2.5YR5/6	m,m,sbk	I	.0	6.6	63.9	19.5	3.2	3.1	3.7	.11	1.62	12.5	.5
								Soil H									
SH-1	Btb	0-20	sl	2.5YR5/7	s,m,sbk	none	0.0	5.3	61.9	20.3	3.9	4.4	4.2	0.14	1.67	5.2	.9
SH-2	Btkb	20-55	sl	2.5YR6/5	m,c,sbk	I	.0	12.6	59.3	15.0	2.9	2.8	7.3	.18	1.72	18.7	1.0
SH-3	Ckmb	55-80	sl	2.5YR6/5	m	II	.0	16.8	58.9	14.3	2.3	2.2	5.5	.14	1.84	16.2	.8
SH-4	2Ckb1	80-95	vgls	2.5YR6/4	m,f,abk	II	66.1	34.8	48.7	11.2	1.8	1.7	1.8	.07	1.92	15.3	1.2
SH-5	3Ckb2	95-120	ls	2.5YR5/5	s,c,sbk	I-	.0	31.6	49.2	12.3	2.1	2.0	2.8	.09	1.82	9.7	.5
								Soil G									
SG-1	Btkb	0-15	sl	2.5YR4/6	m,m,abk	I	0.0	16.8	59.6	10.2	2.3	3.1	7.9	0.20	1.77	9.9	0.7
SG-2	2Ckb1	15-40	vgls	2.5YR5/5	w,m,abk	II	70.0	42.6	38.9	10.4	2.2	1.8	4.0	.10	1.7[e]	15.4	.5
SG-3	2Ckb2	40-140	vgls	2.5YR5/5	m-sg	I	70.5	48.0	36.6	8.9	1.7	1.7	3.1	.08	1.7[e]	11.9	.5
SG-4	2Ckb3	140-180	vgs	2.5YR5/6	m-sg	none	43.1	60.9	26.4	7.8	1.5	1.4	2.0	.06	1.7[e]	11.0	.5

Sample	horizon[1]	Depth (cm)	Texture[2]	Color[3] (dry)	Structure[4]	Carbonate morphology[5]	Weight percent gravel	Sand Coarse	Sand Fine	Silt Coarse	Silt Fine	Clay Coarse	Clay Fine	Total clay (g/cm^3)	Bulk density[7] (g/cm^3)	Percent $CaCO_3$ (<2mm)	Weight loss on ignition
							Soil F										
SF-1	Btb	0-12	sl	2.5YR5/6	m,m,abk	I	0.0	3.2	52.8	25.8	4.4	3.8	10.0	0.23	1.67	7.2	1.1
SF-2	Btkb	12-23	sl	2.5YR6/6	m,m,abk	I+	.0	1.9	50.2	30.0	4.6	3.3	10.0	.22	1.65	10.1	1.0
SF-3	Ckb	23-43	sl	2.5YR6/6	w,m,pr-m,m,abk	II-	.0	7.7	54.0	24.7	3.7	3.0	6.9	.17	1.74	5.1	.9
SF-4	Btb	43-60	sl	2.5YR5/7	w,m,sbk	none	.0	15.7	56.3	12.2	3.0	3.2	9.6	.24	1.83	.5	.9
SF-5	Ckb1	60-96	sl	5YR7/5	w,c,pr-m,m,abk	III	.0	.9	65.3	20.2	3.3	3.6	6.6	.18	1.71	25.6	.8
SF-6	Ckb2	96-116	sl	5YR7/5-2.5YR6/6	m,m,abk	II-	.0	11.2	62.3	14.7	2.4	2.3	7.2	.18	1.84	15.8	.6
SF-7	2Ckb3	116-140	vgsl	2.5YR5/5	w,m,sbk	II+	51.7	29.0	45.5	14.0	2.5	2.4	6.5	.15	1.64	13.8	.5
SF-8	2Ckb4	140-167	vgsl	2.5YR4/6	w,m,abk	II	67.4	39.6	34.9	9.9	2.3	3.3	9.9	.24	1.74	13.0	.7
							Soil E										
SE-1	Bkb	0-20	vgls	2.5YR4/6	w,f,sbk	none	45.5	57.9	24.7	7.7	1.4	0.9	7.4	0.17	1.99	7.7	0.5
SE-2	2Btb	20-35	scl	10YR4/6	s,m,abk	none	.0	17.1	45.4	10.9	2.4	3.6	20.7	.46	1.89	.5	1.2
SE-3	2Btkb	35-48	sl	2.5YR5/6 2.5YR6/6[b]	s,m,abk	II	.0	15.9	49.6	15.9	3.0	3.6	12.0	.29	1.85	11.7	1.0
SE-4	2Ckb1	48-74	sl	2.5YR6/6	s,f,abk	III-	.0	14.7	49.8	20.3	3.2	2.2	9.8	.23	1.87	16.6	.7
SE-5	2Ckb2	74-126	sl	2.5YR6/6	m,c,pl	III-	.0	12.8	53.3	20.1	3.4	2.6	7.7	.19	1.85	14.6	.8
SE-6	2Ckb3	126-156	l	2.5YR5/6	m	II-	.0	3.6	42.2	32.7	7.3	4.0	10.3	.24	1.68	11.8	1.0
							Soil D										
SD-3	Ckb1	0-40	sl	n.d.	n.d.	I+	0.0	7.1	50.3	27.4	4.0	2.8	8.5	0.20	1.79	11.8	0.8
SD-2	Ckb2	40-80	sl	n.d.	n.d.	I+	.0	9.2	45.6	26.5	4.8	3.0	10.8	.25	1.81	9.1	1.3
SD-1	Ckb3	0-20	l	n.d.	n.d.	I-II	.0	4.8	38.2	36.5	7.2	5.4	7.9	.23	1.74	14.1	1.5
							Soil C										
SC-1	Btkb1	0-35	sl	2.5YR4/6	s,m,abk	I	0.0	11.1	56.1	20.2	4.0	4.2	4.3	0.16	1.87	3.9	1.1
SC-2	Btkb2	35-55	sl	2.5YR4/7	m,f,abk	I	.0	12.1	53.3	19.2	3.3	3.9	8.1	.23	1.86	8.9	1.1
SC-3	CBkb	55-78	sl	5YR4/6 5YR6/4[b]	s,m,abk	III-	.0	8.1	49.1	24.9	4.5	4.4	8.9	.24	1.80	25.1	1.1
SC-4	Ckb1	78-114	sl	5YR5/4	m,m,abk	II	.0	9.1	45.9	28.9	4.6	2.8	8.7	.20	1.76	21.3	1.0
SC-5	Ckb2	114-150	sl	5YR4/7	w,c,abk	I	.0	6.7	48.9	29.0	4.8	3.5	7.0	.19	1.8[e]	15.8	.8
SC-6	Ckb3	150-190	sl	5YR4/6	w,c,abk	none	.0	6.0	48.9	28.4	5.6	4.3	6.9	.20	1.79	11.2	.8

Table 4. Soil descriptions and laboratory data, Fisher Valley soils—Continued

Sample	horizon[1]	Depth (cm)	Texture[2]	Color[3] (dry)	Structure[4]	Carbonate morphology[5]	Weight percent gravel	Weight percent[6] Sand Coarse	Fine	Silt Coarse	Fine	Clay Coarse	Fine	Total clay (g/cm³)	Bulk density[7] (g/cm³)	Percent CaCO3 (<2mm)	Weight loss on ignition
								Soil B									
SB-1	BAkb	0-12	sl	5YR4/8	w,m,abk	I	0.0	21.0	51.8	16.0	3.0	2.4	5.8	0.16	1.91	11.9	0.9
SB-2	Bkb	12-22	sl	5YR5/8	m,c,abk	I	.0	24.7	47.7	17.4	3.4	2.3	4.5	.13	1.91	12.8	.8
SB-3	Btkb1	22-40	sl	5YR5/7	s,m,abk	II	.0	10.4	45.9	27.2	5.7	3.8	6.9	.21	1.90	18.6	1.0
SB-4	Btkb2	40-80	l	5YR5/8	m-s,m,abk	I	.0	6.1	38.2	32.7	8.6	4.7	9.7	.27	1.84	12.2	1.1
SB-5	Ckb	80-90	sl	2.5YR4/7	w,m,abk	I	.0	7.8	52.1	24.7	4.4	3.3	7.7	.19	1.76	10.3	.9
								Soil A									
SA-2	BAb	10-21	sl	5YR5/8	w,m,abk	none	0.0	3.7	68.1	17.9	2.5	2.3	5.4	0.14	1.78	2.2	0.7
SA-3	Bwb	21-41	sl	5YR5/7	s,c,abk	none	.0	4.4	72.5	10.7	1.9	2.7	7.8	.19	1.80	1.0	.9
SA-4	Btkb	41-85	l	5YR5/8	s,m,abk	II	.0	2.2	42.5	31.7	7.7	4.4	11.5	.31	1.90	16.3	1.3
SA-5	Ckb1	85-114	sl	5YR5/7	s,m,abk	I	.0	2.2	55.3	25.4	5.3	3.5	8.3	.22	1.89	9.5	1.2
SA-6	Ckb2	114-150	sl	5YR5/7	m,c,abk	I	.0	2.1	51.6	27.0	5.9	3.5	9.8	.25	1.89	11.3	.9
SA-7	Ckb3	150-170	sl	5YR5/8	w,c,abk	I	.0	4.5	59.0	22.7	4.4	3.2	6.3	.18	1.86	10.3	.8
								Soil I (gravelly facies)									
s1	BAkb	0-18	sl	7.5YR5/6	m,m,sbk	none	0.0	3.0	63.5	20.2	3.6	3.8	5.8	0.16	1.63	12.9	2.4
s2	Btkb	18-38	sl	5YR6/6	m,f,abk	II-	.0	2.8	62.4	16.4	4.2	4.3	9.9	.25	1.71	20.1	2.7
s3	KBb	38-58	vgsl	5YR8/4	s,m,abk	III	58.3	2.8	54.3	23.4	3.5	2.6	13.4	.30	1.87	54.8	3.5
s4	2Kmb1	58-89	vgs	5YR7/5	s,m,pl	IV	93.4	n.d.	n.d.	n.d.	n.d.	n.d.	n.d.	n.d.	2.01	47.6	3.5
s5	2Kmb2	89-129	vgs	5YR7/4	m to w,f,pl	III	92.8	n.d.	n.d.	n.d.	n.d.	n.d.	n.d.	n.d.	2.01	22.3	2.0
s6	2Kmb3	129-159	vgs	5YR7/4	m to w,f,pl	III	59.7	46.4	44.7	7.5	1.2	.1	.1	.00	1.91	18.6	1.3
s7	2Ckb	159-189	vgls	2.5YR5/6	sg	none	50.1	56.5	28.0	10.9	2.5	1.3	.8	.04	1.7e	12.1	.7

[1] Horizon nomenclature from Birkeland (1983) and Guthrie and Witty (1982).

[2] Texture: s, sand; l, loam; sl, sandy loam; ls, loamy sand; scl, sandy clay loam; g, gravelly, 15-35 percent gravel by weight; vg, very gravelly, >35 percent gravel by weight.

[3] Color, Munsell Color System: a, mottles; b, burrows; all others matrix.

[4] Structure: grade, size, type. Grade: w, weak; m, moderate; s, strong. Size: vf, very fine; f, fine; m, medium; c, coarse. Type: abk, angular blocky; sbk, subangular blocky; pl, platy; m, massive; sg, single grain.

[5] Roman numerals are stages (Machette, 1985).

[6] Percentages are of sample fraction < 2mm. Grain-size intervals: coarse sand, 0.25-2.0 mm; fine sand, 0.05-0.25 mm; coarse silt, 0.01-0.05 mm; fine silt, 0.002-0.01 mm; coarse clay, 0.0005-0.002 mm; fine clay, <0.0005 mm.

[7] e, estimated.

Table 5. Secondary carbonate in Fisher Valley soils

[--, not applicable]

Sample	Horizon	Thickness (cm)	Less than 2 mm fraction						Greater than 2 mm fraction						Total secondary CaCO$_3$ (g/cm^2)
				Present		Original[2]				Present		Original[2]			
			Weight percent	Bulk density[1] (g/cm^3)	Percent CaCO$_3$	Bulk density (g/cm^3)	Percent CaCO$_3$	Secondary CaCO$_3$ (g/cm^3)	Weight percent	Bulk density[3] (g/cm^3)	Percent CaCO$_3$	Bulk density (g/cm^3)	Percent CaCO$_3$	Secondary CaCO$_3$ (g/cm^3)	
								Soil J							
SJ-1	A1	8	100.0	1.4[e]	6.7	1.4	7.0	-0.004	0.0	--	--	--	--	--	0.0
SJ-2	A1	10	100.0	1.43	6.4	1.4	7.0	-0.006	.0	--	--	--	--	--	-0.1
SJ-3	Ck1	24	100.0	1.47	8.4	1.4	7.0	.025	.0	--	--	--	--	--	.6
SJ-4	Ck2	30	100.0	1.43	7.6	1.4	7.0	.011	.0	--	--	--	--	--	.3
								Soil I							
SI-1	Btb	20	100.0	1.76	0.6	1.6	9.0	-0.13	0.0	--	--	--	--	--	-2.6
SI-2	Btkb1	23	100.0	1.81	1.2	1.6	9.0	-0.12	.0	--	--	--	--	--	-2.8
SI-3	Btkb2	24	100.0	1.82	2.3	1.6	9.0	-0.10	.0	--	--	--	--	--	-2.4
SI-4	BKb	26	100.0	1.68	3.1	1.6	9.0	-0.092	.0	--	--	--	--	--	-2.4
SI-5	KBb	16	100.0	1.72	39.4	1.6	9.0	.53	.0	--	--	--	--	--	8.5
SI-6	Kb1	26	100.0	1.69	37.0	1.6	9.0	.48	.0	--	--	--	--	--	12.5
SI-7	Kb2	35	100.0	1.91	24.5	1.6	9.0	.32	.0	--	--	--	--	--	11.2
SI-8	Ckb1	48	100.0	1.89	18.2	1.6	9.0	.20	.0	--	--	--	--	--	9.6
SI-9	Ckb2	30	100.0	1.81	12.0	1.6	9.0	.073	.0	--	--	--	--	--	2.1
SI-10	Ckb3	34	100.0	1.81	14.4	1.6	9.0	.12	.0	--	--	--	--	--	4.1
SI-11	Ckb4	35	100.0	1.62	12.5	1.6	9.0	.059	.0	--	--	--	--	--	2.1
															39.8
								Soil H							
SH-1	Btb	20	100.0	1.67	5.2	1.6	9.0	-0.057	0.0	--	--	--	--	--	-1.1
SH-2	Btkb	35	100.0	1.72	18.7	1.6	9.0	.18	.0	--	--	--	--	--	6.3
SH-3	Ckmb	25	100.0	1.84	16.2	1.6	9.0	.15	.0	--	--	--	--	--	3.8
SH-4	2Ckb1	15	33.9	1.92	15.3	1.6	9.0	.15	66.1	2.2	18.9	2.2	12.0	.15	2.3
SH-5	3Ckb2	25	100.0	1.82	9.7	1.6	9.0	.033	.0	--	--	--	--	--	.8
															12.1
								Soil G							
SG-1	Btkb	15	100.0	1.77	9.9	1.6	9.0	0.031	0.0	--	--	--	--	--	0.5
SG-2	2Ckb1	25	30.0	1.7[e]	15.4	1.6	9.0	.12	70.0	2.2	15.1	2.2	12.0	.068	2.1
SG-3	2Ckb2	100	29.5	1.7[e]	11.9	1.6	9.0	.058	70.5	2.2	12.4	2.2	12.0	.009	2.3
SG-4	2Ckb3	40	56.9	1.7[e]	11.0	1.6	9.0	.043	43.1	2.2	17.9	2.2	12.0	.13	3.2
															8.1

Table 5. Secondary carbonate in Fisher Valley soils—Continued

Sample	Horizon	Thickness (cm)	Less than 2 mm fraction						Greater than 2 mm fraction						Total secondary CaCO$_3$ (g/cm^2)
			Weight percent	Present		Original[2]		Secondary CaCO$_3$ (g/cm^3)	Weight percent	Present		Original[2]		Secondary CaCO$_3$ (g/cm^3)	
				Bulk density[1] (g/cm^3)	Percent CaCO$_3$	Bulk density (g/cm^3)	Percent CaCO$_3$			Bulk density[3] (g/cm^3)	Percent CaCO$_3$	Bulk density (g/cm^3)	Percent CaCO$_3$		
								Soil F							
SF-1	Btb	12	100.0	1.67	7.2	1.6	9.0	-0.024	0.0	--	--	--	--	--	-0.3
SF-2	Btkb	11	100.0	1.65	10.1	1.6	9.0	.023	.0	--	--	--	--	--	.3
SF-3	Ckb	20	100.0	1.74	5.1	1.6	9.0	-0.055	.0	--	--	--	--	--	-1.1
SF-4	Btb	17	100.0	1.83	.5	1.6	9.0	-0.14	.0	--	--	--	--	--	-2.4
SF-5	Ckbl	36	100.0	1.71	25.6	1.6	9.0	.29	.0	--	--	--	--	--	10.4
SF-6	Ckb2	20	100.0	1.84	15.8	1.6	9.0	.15	.0	--	--	--	--	--	3.0
SF-7	2Ckb3	24	43.8	1.64	13.8	1.6	9.0	.082	51.7	2.2	9.3	2.2	9.3	.00	.9
SF-8	2Ckb4	27	32.6	1.74	13.0	1.6	9.0	.082	67.4	2.2	15.1	2.2	12.0	.068	2.0
															13.0
								Soil E							
SE-1	Bkb	20	54.5	1.99	7.7	1.6	9.0	0.009	45.5	2.2	19.2	2.2	12.0	0.16	1.6
SE-2	2Btb	15	100.0	1.89	.5	1.6	9.0	-0.14	.0	--	--	--	--	--	-2.1
SE-3	2Btkb	13	100.0	1.85	11.7	1.6	9.0	.072	.0	--	--	--	--	--	.9
SE-4	2Ckbl	26	100.0	1.87	16.6	1.6	9.0	.17	.0	--	--	--	--	--	4.4
SE-5	2Ckb2	52	100.0	1.85	14.6	1.6	9.0	.13	.0	--	--	--	--	--	6.8
SE-6	2Ckb3	30	100.0	1.68	11.8	1.6	9.0	.054	.0	--	--	--	--	--	1.6
															13.2
								Soil D							
SD-3	Ckbl	40	100.0	1.79	11.8	1.6	9.0	0.067	0.0	--	--	--	--	--	2.7
SD-2	Ckb2	40	100.0	1.81	9.1	1.6	9.0	.021	.0	--	--	--	--	--	.8
SD-1	Ckb3	20	100.0	1.74	14.1	1.6	9.0	.10	.0	--	--	--	--	--	2.0
															5.5
								Soil C							
SC-1	Btkbl	35	100.0	1.87	3.9	1.6	9.0	-0.071	0.0	--	--	--	--	--	-2.5
SC-2	Btkb2	20	100.0	1.86	8.9	1.6	9.0	.022	.0	--	--	--	--	--	.4
SC-3	CBkb	23	100.0	1.80	25.1	1.6	9.0	.31	.0	--	--	--	--	--	7.1
SC-4	Ckbl	36	100.0	1.76	21.3	1.6	9.0	.23	.0	--	--	--	--	--	8.3
SC-5	Ckb2	36	100.0	1.8[e]	15.8	1.6	9.0	.14	.0	--	--	--	--	--	5.0
SC-6	Ckb3	40	100.0	1.79	11.2	1.6	9.0	.056	.0	--	--	--	--	--	2.2
															20.5

| | | | Less than 2 mm fraction | | | | | | Greater than 2 mm fraction | | | | | | Total |
Sample	Horizon	Thickness (cm)	Weight percent	Present Bulk density[1] (g/cm^3)	Present Percent CaCO$_3$	Original[2] Bulk density (g/cm^3)	Original[2] Percent CaCO$_3$	Secondary CaCO$_3$ (g/cm^3)	Weight percent	Present Bulk density[3] (g/cm^3)	Present Percent CaCO$_3$	Original[2] Bulk density (g/cm^3)	Original[2] Percent CaCO$_3$	Secondary CaCO$_3$ (g/cm^3)	secondary CaCO$_3$ (g/cm^2)
								Soil B							
SB-1	BAkb	12	100.0	1.91	11.9	1.6	9.0	0.083	0.0	--	--	--	--	--	1.0
SB-2	Bkb	10	100.0	1.91	12.8	1.6	9.0	.10	.0	--	--	--	--	--	1.0
SB-3	Btkb1	18	100.0	1.90	18.6	1.6	9.0	.21	.0	--	--	--	--	--	3.8
SB-4	Btkb2	40	100.0	1.84	12.2	1.6	9.0	.080	.0	--	--	--	--	--	3.2
SB-5	Ckb	10	100.0	1.76	10.3	1.6	9.0	.037	.0	--	--	--	--	--	.4
															9.4
								Soil A							
SA-2	BAb	11	100.0	1.78	2.2	1.6	9.0	-0.11	0.0	--	--	--	--	--	-1.2
SA-3	Bwb	20	100.0	1.80	1.0	1.6	9.0	-0.13	.0	--	--	--	--	--	-2.6
SA-4	Btkb	44	100.0	1.90	16.3	1.6	9.0	.17	.0	--	--	--	--	--	7.5
SA-5	Ckb1	29	100.0	1.89	9.5	1.6	9.0	.036	.0	--	--	--	--	--	1.0
SA-6	Ckb2	36	100.0	1.89	11.3	1.6	9.0	.070	.0	--	--	--	--	--	2.5
SA-7	Ckb3	20	100.0	1.86	10.3	1.6	9.0	.049	.0	--	--	--	--	--	1.0
															8.2
								Soil I (gravelly facies)							
s1	BAkb	18	100.0	1.63	12.9	1.6	9.0	0.066	0.0	--	--	--	--	--	1.2
s2	Btkb	20	100.0	1.71	20.1	1.6	9.0	.20	.0	--	--	--	--	--	4.0
s3	KBb	20	41.7	1.87	54.8	1.6	9.0	.88	58.3	2.2	69.4	2.2	12.0	1.26	22.0
s4	2Kmb1	31	6.6	2.01	47.6	1.6	9.0	.81	93.4	2.2	32.0	2.2	12.0	.44	14.4
s5	2Kmb2	40	7.2	2.01	22.3	1.6	9.0	.30	92.8	2.2	22.3	2.2	12.0	.23	9.4
s6	2Kmb3	30	40.3	1.91	18.6	1.6	9.0	.21	59.7	2.2	21.5	2.2	12.0	.21	6.3
s7	2Ckb	30	49.9	1.7^e	12.1	1.6	9.0	.062	50.1	2.2	17.5	2.2	12.0	.12	2.7
															60.0

[1] e, estimated.

[2] Original properties (bulk density, percent CaCO$_3$) estimated from soil parent materials and young similar deposits.

[3] Estimates, based on gravel lithology.

Table 6. Secondary clay in Fisher Valley soils

[n.d., not determined]

Sample	Horizon	Thickness (cm)	Weight percent < 2 mm	Present Bulk density[1] (g/cm^3)	Present Percent clay	Original[2] Bulk density (g/cm^3)	Original[2] Percent clay	Secondary clay (g/cm^3)	Total secondary clay (g/cm^2)
				Soil J					
SJ-1	A1	8	100.0	1.4^e	10.5	1.4	5.0	0.077	0.6
SJ-2	A1	10	100.0	1.43	13.3	1.4	5.0	.12	1.2
SJ-3	Ck1	24	100.0	1.47	6.3	1.4	5.0	.023	.6
SJ-4	Ck2	30	100.0	1.43	5.6	1.4	5.0	.010	.3
									2.7
				Soil I					
SI-1	Btb	20	100.0	1.76	16.0	1.6	6.2	0.18	3.6
SI-2	Btkb1	23	100.0	1.81	19.1	1.6	6.2	.25	5.8
SI-3	Btkb2	24	100.0	1.82	21.3	1.6	6.2	.29	7.0
SI-4	BKb	26	100.0	1.68	16.2	1.6	6.2	.17	4.4
SI-5	KBb	16	100.0	1.72	18.1	1.6	6.2	.21	3.4
SI-6	Kb1	26	100.0	1.69	14.4	1.6	6.2	.14	3.6
SI-7	Kb2	35	100.0	1.91	12.0	1.6	6.2	.13	4.6
SI-8	Ckb1	48	100.0	1.89	7.1	1.6	6.2	.035	1.7
SI-9	Ckb2	30	100.0	1.81	6.2	1.6	6.2	.013	.4
SI-10	Ckb3	34	100.0	1.81	7.1	1.6	6.2	.029	1.0
SI-11	Ckb4	35	100.0	1.62	6.8	1.6	6.2	.011	.4
									35.9
				Soil H					
SH-1	Btb	20	100.0	1.67	8.6	1.6	3.5	0.088	1.8
SH-2	Btkb	35	100.0	1.72	10.1	1.6	3.5	.12	4.2
SH-3	Ckmb	25	100.0	1.84	7.7	1.6	3.5	.086	2.1
SH-4	2Ckb1	15	33.9	1.92	3.5	1.6	3.5	.011	.1
SH-5	3Ckb2	25	100.0	1.82	4.8	1.6	3.5	.031	.8
									9.0
				Soil G					
SG-1	Btkb	15	100.0	1.77	11.0	1.6	3.4	0.14	2.1
SG-2	2Ckb1	25	30.0	1.7^e	5.8	1.6	3.4	.044	.3
SG-3	2Ckb2	100	29.5	1.7^e	4.8	1.6	3.4	.027	.8
SG-4	2Ckb3	40	56.9	1.7^e	3.4	1.6	3.4	.003	.1
									3.3
				Soil J					
SF-1	Btb	12	100.0	1.67	13.8	1.6	8.9	0.088	1.1
SF-2	Btkb	11	100.0	1.65	13.3	1.6	8.9	.077	.8
SF-3	Ckb	20	100.0	1.74	9.9	1.6	8.9	.030	.6
SF-4	Btb	17	100.0	1.83	12.8	1.6	8.9	.092	1.6
SF-5	Ckb1	36	100.0	1.71	10.2	1.6	8.9	.032	1.2
SF-6	Ckb2	20	100.0	1.84	9.5	1.6	8.9	.032	.6
SF-7	2Ckb3	24	43.8	1.64	8.9	1.6	8.9	.004	.1
SF-8	2Ckb4	27	32.6	1.74	13.2	1.6	8.9	.087	.8
									6.8

Table 6. Secondary clay in Fisher Valley soils—Continued

Sample	Horizon	Thickness (cm)	Weight percent < 2 mm	Present Bulk density[1] (g/cm³)	Present Percent clay	Original[2] Bulk density (g/cm³)	Original[2] Percent clay	Secondary clay (g/cm³)	Total secondary clay (g/cm²)
				Soil E					
SE-1	Bkb	20	54.5	1.99	8.3	1.6	9.0	0.021	0.2
SE-2	2Btb	15	100.0	1.89	24.3	1.6	9.0	.32	4.8
SE-3	2Btkb	13	100.0	1.85	15.6	1.6	9.0	.15	2.0
SE-4	2Ckb1	26	100.0	1.87	12.0	1.6	9.0	.080	2.1
SE-5	2Ckb2	52	100.0	1.85	10.3	1.6	9.0	.047	2.4
SE-6	2Ckb3	30	100.0	1.68	14.3	1.6	9.0	.096	2.9
									14.4
				Soil C					
SC-1	Btkb1	35	100.0	1.87	8.5	1.6	9.0	0.015	0.5
SC-2	Btkb2	20	100.0	1.86	12.0	1.6	9.0	.079	1.6
SC-3	CBkb	23	100.0	1.80	13.3	1.6	9.0	.095	2.2
SC-4	Ckb1	36	100.0	1.76	11.5	1.6	9.0	.058	2.1
SC-5	Ckb2	36	100.0	1.8e	10.5	1.6	9.0	.045	1.6
SC-6	Ckb3	40	100.0	1.79	11.2	1.6	9.0	.056	2.2
									10.2
				Soil B					
SB-1	BAkb	12	100.0	1.91	8.2	1.6	9.0	0.013	0.2
SB-2	Bkb	10	100.0	1.91	6.8	1.6	9.0	.000	.0
SB-3	Btkb1	18	100.0	1.90	10.7	1.6	9.0	.059	1.1
SB-4	Btkb2	40	100.0	1.84	14.4	1.6	9.0	.12	4.8
SB-5	Ckb	10	100.0	1.76	11.0	1.6	9.0	.050	.5
									6.6
				Soil A					
SA-2	BAb	11	100.0	1.78	7.7	1.6	9.0	0.00	0.0
SA-3	Bwb	20	100.0	1.80	10.5	1.6	9.0	.045	.9
SA-4	Btkb	44	100.0	1.90	15.9	1.6	9.0	.16	7.0
SA-5	Ckb1	29	100.0	1.89	11.8	1.6	9.0	.079	2.3
SA-6	Ckb2	36	100.0	1.89	13.3	1.6	9.0	.11	4.0
SA-7	Ckb3	20	100.0	1.86	9.5	1.6	9.0	.033	.7
									14.9
				Soil I (gravelly facies)					
s1	BAkb	18	100.0	1.63	9.6	1.6	2.0	0.12	2.2
s2	Btkb	20	100.0	1.71	14.2	1.6	2.0	.21	4.2
s3	KBb	20	41.7	1.87	16.0	1.6	2.0	.27	2.3
s4	2Kmb1	31	6.6	2.01	n.d.	1.6	2.0	n.d.	n.d.
s5	2Kmb2	40	7.2	2.01	n.d.	1.6	2.0	n.d.	n.d.
s6	2Kmb3	30	40.3	1.91	.2	1.6	2.0	.000	.0
s7	2Ckb	30	49.9	1.7e	2.1	1.6	2.0	.004	.1
									8.8

[1] e, estimated.

[2] Original properties (bulk density, percent clay) estimated from soil parent materials and young similar deposits.